



HAL
open science

Nanomedicines functionalized with anti-EGFR ligands for active targeting in cancer therapy: Biological strategy, design and quality control

Phuoc Vinh Nguyen, Emilie Allard-Vannier, Igor Chourpa, Katel Hervé-Aubert

► To cite this version:

Phuoc Vinh Nguyen, Emilie Allard-Vannier, Igor Chourpa, Katel Hervé-Aubert. Nanomedicines functionalized with anti-EGFR ligands for active targeting in cancer therapy: Biological strategy, design and quality control. *International Journal of Pharmaceutics*, 2021, 605, pp.120795. 10.1016/j.ijpharm.2021.120795 . hal-03266148

HAL Id: hal-03266148

<https://univ-tours.hal.science/hal-03266148v1>

Submitted on 2 Aug 2023

HAL is a multi-disciplinary open access archive for the deposit and dissemination of scientific research documents, whether they are published or not. The documents may come from teaching and research institutions in France or abroad, or from public or private research centers.

L'archive ouverte pluridisciplinaire **HAL**, est destinée au dépôt et à la diffusion de documents scientifiques de niveau recherche, publiés ou non, émanant des établissements d'enseignement et de recherche français ou étrangers, des laboratoires publics ou privés.



Distributed under a Creative Commons Attribution - NonCommercial 4.0 International License

Nanomedicines functionalized with anti-EGFR ligands for active targeting in cancer therapy: biological strategy, design and quality control

Phuoc Vinh Nguyen, Emilie Allard-Vannier, Igor Chourpa, Katel Hervé-Aubert*

* EA6295 Nanomédicaments et Nanosondes, Université de Tours, Tours, France

Abstract

Recently, active targeting using nanocarriers with biological ligands has emerged as a novel strategy for improving the delivery of therapeutic and/or imaging agents to tumor cells. The presence of active targeting moieties on the surface of nanomedicines has been shown to play an important role in enhancing their accumulation in tumoral cells and tissues versus healthy ones. This property not only helps to increase the therapeutic index but also to minimize possible side effects of the designed nanocarriers. Since the overexpression of epidermal growth factor receptors (EGFR) is a common occurrence linked to the progression of a broad variety of cancers, the potential application of anti-EGFR immunotherapy and EGFR-targeting ligands in active targeting nanomedicines is getting increasing attention. Henceforth, the EGFR-targeted nanomedicines were extensively studied *in vitro* and *in vivo* but exhibited both satisfactory and disappointing results, depending on used protocols. This review is designed to give an overview of a variety of EGFR-targeting ligands available for nanomedicines, how to conjugate them onto the surface of nanoparticles, and the main analytical methods to confirm this successful conjugation.

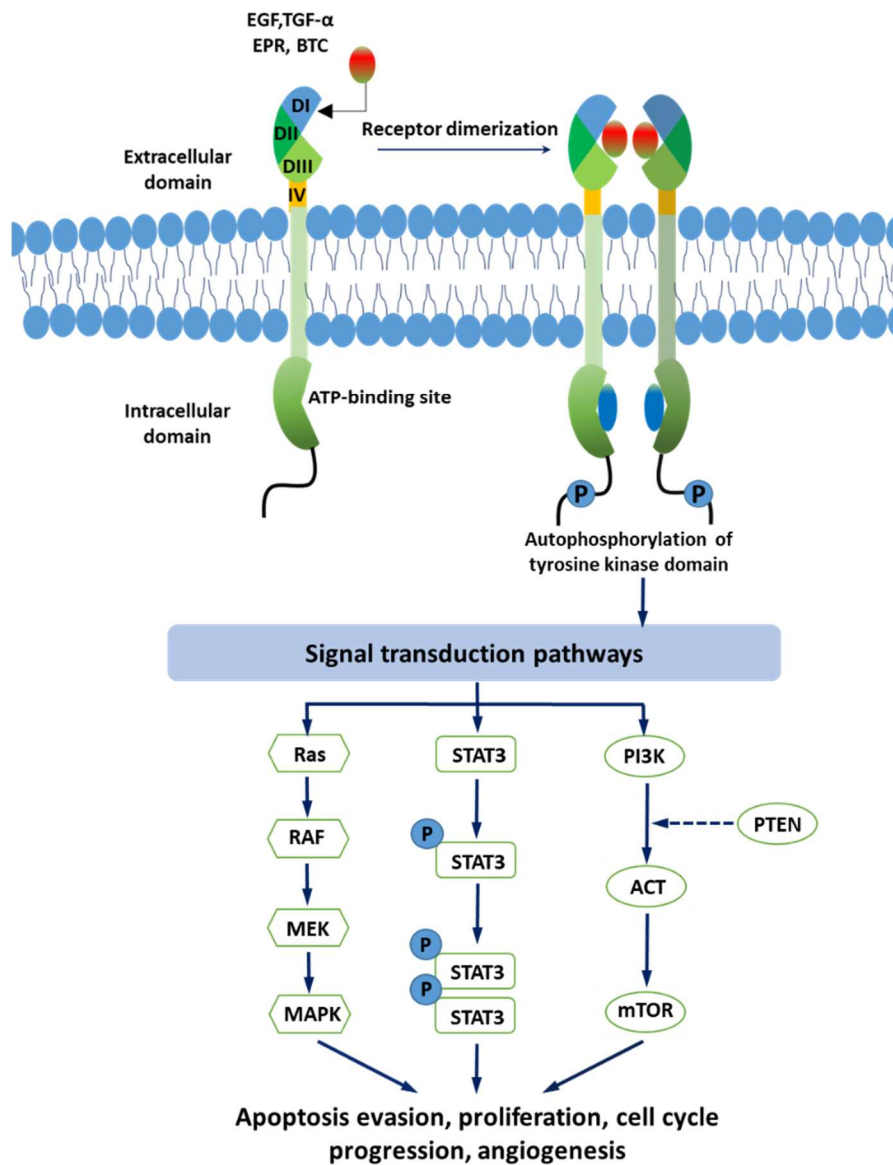
Keywords: EGFR; nanomedicine; active targeting; cancer therapy; biological ligands

1. Epidermal Growth Factor Receptor (EGFR) and its role in tumor development

The epidermal growth factor receptor (EGFR/ErbB1/HER1) is a 170 kDa transmembrane glycoprotein of the tyrosine kinase family, which comprises HER1; HER2; HER3 and HER4. This protein is a single polypeptide chain of 1186 amino acid residues and a substantial amount of N-linked oligosaccharides, which divide an EGFR into three principal domains including an extracellular ligand-binding domain, a single hydrophobic transmembrane domain and a cytoplasmic tyrosine kinase (Fig. 1). On one side, the intracellular domain is highly conserved, typical for the family and helps distinguish EGFRs from other receptors in the same family. On the other hand, the extracellular domain is less conserved and allows EGFRs to bind to different ligands. The extracellular domain consists of four smaller segments from DI to DIV. DI and DIII are essential in the ligand-binding process, whereas DII and DIV constitute the disulfide bond (De Luca *et al.*, 2008; Grapa *et al.*, 2019; Sasaki *et al.*, 2013).

The activation of an EGFR occurs when its ligand binds to its extracellular domain. There are several natural mammalian ligands for EGFRs including the epidermal growth factor protein (EGF), the transforming growth factor- α (TGF- α), epiregulin (EPR), betacellulin (BTC), and EGFR-like growth factors. As shown in the Fig. 1, once the ligand binds to an EGFR, the dimerization and the phosphorylation of the cytoplasmic domain will occur and lead to a cascade of subsequent downstream processes including the phosphatidylinositol-3-kinase (PI3K) pathway, the signal transducer and activator of transcription 3 (STAT3) pathway, and the Ras-Raf-MAPK pathway (Grapa *et al.*, 2019; Sasaki *et al.*, 2013).

44 In normal cells, EGFRs play an important role in two main signal pathways of cell proliferation. Their
 45 expression is tightly regulated to ensure that the kinetics of cell proliferation corresponds to the
 46 tissues' requirement for homeostasis. On the contrary, in cancer cells, EGFRs are often perpetually
 47 stimulated. The EGFR overexpression has been found to be correlated to multiple cancer-related
 48 signaling pathways and contributes significantly to chemotherapy/radiotherapy resistance,
 49 angiogenesis, and apoptosis (Grapa *et al.*, 2019; Sasaki *et al.*, 2013). The expression level of EGFRs in
 50 ordinary and cancer cells is defined at 4.0-10.0 ($\times 10^4$) and over 10^6 EGFRs, respectively (Akbarzadeh
 51 Khiavi *et al.*, 2020). To determine the EGFR expression level, several methods can be used such as the
 52 analysis of DNA, RNA, the protein level or the assessment of the degree of receptors by analyzing the
 53 receptor activation or downstream markers. Among these methods, immunohistochemistry (IHC) is
 54 the most widely used method for clinical samples (Ciardiello and Tortora, 2003). The EGFR
 55 overexpression has been found to be related to poor prognosis in a variety of human solid tumors
 56 such as non-small cell lung, head and neck, colorectal, pancreas, breast, ovary, and bladder and
 57 kidney cancers. Table 1 gives information on the expression rate of EGFRs in these cancers and the
 58 EGFR-overexpressing cancer cell lines that are usually used in research.



59

60

Fig. 1. EGFR structure and EGFR signaling pathways

61 **Table 1. Types of cancer with EGFR overexpression and cancer cell lines used in preclinical studies**

Type of cancer	Cancer cell line used in research	EGFR overexpression rate (%)	References
Non-small cell lung cancer	A549; H322; H358; H460; H1299; H1975	40-80	(Jorge et al., 2014; Master and Sen Gupta, 2012; Yoon et al., 2016)
Squamous-cell carcinoma of head and neck cancer	UM-SCC-14C, UM-SCC-22A, SCCVII	80-100	(Altintas et al., 2013; Master and Sen Gupta, 2012; ping et al., 2010; Zimmermann et al., 2006)
Colorectal cancer	Caco-2, HT-29, SW480, SW403, SW620, HCT116, HCT-8	25-77	(Krasinskas, 2011; Li et al., 2019; Master and Sen Gupta, 2012; Z. Zhang et al., 2018)
Pancreatic cancer	Pan-1, Capan-1	30-89	(Du et al., 2018; Grapa et al., 2019; Xu et al., 2013)
Breast cancer	MDA-MB-468, MDA-MB-231, MCF-7	15-45	(Brinkman et al., 2016; Changavi et al., 2015; Jin et al., 2017; Kim et al., 2017)
Ovarian cancer	SKOV-3	4-100	(Chen et al., 2017; Teplinsky and Muggia, 2015)
Bladder and kidney cancer	MBT-2	31-46	(Li et al., 2018)
Gastric cancer	MKN45	27-64	(Arienti et al., 2019; Tsai et al., 2018)

62

63 Considering the involvement of EGFRs in diverse cancer cellular processes, EGFRs appear as an
 64 interesting target for therapeutic intervention. Thus, a number of strategies have been developed to
 65 target and/or inhibit the EGFR expression. As therapeutic agents, monoclonal antibodies (mAb) and
 66 tyrosine kinase inhibitors (TKI) are being employed to inhibit EGFR expression. Anti-EGFR mAbs such
 67 as cetuximab bind to the extracellular domain and prevent the dimerization process, whereas TKIs
 68 including gefitinib, erlotinib, lapatinib block the proliferation signaling by targeting the intracellular
 69 TK domain. However, the use of anti-EGFR agents as therapeutic agents has demonstrated both
 70 satisfactory and disappointing results in clinical trials (Akbarzadeh Khiavi et al., 2020).

71 On the other hand, nanoparticles (NPs) functionalized with active targeting ligands are more and
 72 more developed and have emerged as one of the most promising strategies for cancer treatment.
 73 Not surprisingly, EGFRs appear among the most targeted receptors in active targeting nanomedicines.
 74 The following sections will be specifically focused on the application of EGFR-targeting molecules not
 75 as therapeutic agents but as targeting ligands for nanoscale-targeted systems.

76 **2. EGFR-targeting ligands for active targeting nanomedicine**

77 Since its discovery, the active targeting in nanomedicines has proved its potency to achieve high
78 targeting specificity, drug delivery efficiency, and to avoid nonspecific binding. These properties not
79 only help improve the therapeutic index due to a higher tumor accumulation of encapsulated
80 therapeutic agents but also attenuate severe side effects that may improve the tolerance of patients
81 with anti-cancer adjuvants' treatment. As a result, several targeting moieties have been developed
82 and can be classified into four main groups including proteins (mainly mAbs and mAbs fragments),
83 peptides, nucleic acids (aptamers), and small molecules (Yu *et al.*, 2012). This section is focused on
84 different EGFR-targeting moieties used for active targeting with nanoparticles (NPs) as well as their
85 potential benefits and drawbacks.

86 **2.1. Epidermal growth factor protein and its derivatives**

87 The epidermal growth factor (EGF) protein is the natural molecule that innately binds to EGFRs. The
88 EGF-EGFR binding leads to receptor internalization via the clathrin-mediated endocytosis pathway.
89 Significant efforts have been carried out to investigate the application of EGF-EGFR recognition to
90 target cancer cells for diagnostic and therapeutic purposes with nanomedicines (Master and Sen
91 Gupta, 2012).

92 **2.1.1. EGF protein**

93 The EGF protein was firstly isolated from the parotid gland of male mice and then from the urine for
94 the human EGF. This protein is considered as a "urogastron" due to its ability to inhibit gastric acid
95 secretion in human. The biological activity of the human EGF overlaps with that of the murine EGF
96 (Nakagawa *et al.*, 1985; Sandoval *et al.*, 2012). It is reported that EGF proteins can prompt abundant
97 effects on both cells and epithelial tissues. Moreover, EGF proteins have various effects on cell
98 regeneration processes including the stimulation of proliferation, the migration of keratinocytes, the
99 formation of granulation tissues, and the stimulation of fibroblast motility.

100 Structurally, an EGF is a single polypeptide consisting of 53 amino acids with a molecular weight (MW)
101 of 6 kDa (Table 2). An EGF protein possesses six cysteine residues forming three internal disulfides,
102 which might be used for further conjugation with NPs. Its binding affinity to EGFRs as reflected by the
103 dissociation constant (K_d) is determined to be from 1.0 to 2.0 nM. Nowadays, several methods can be
104 used to produce EGF proteins in industry such as recombinant DNA methods in animals, bacteria,
105 yeasts and adenoviral vectors (Negahdari *et al.*, 2016).

106 As targeting ligands, the EGF protein is one of the most widely used ligands for EGFR-targeting. The
107 functionalization of NPs with EGFs offers numerous advantages such as: i) a smaller size than that of
108 antibodies (6 kDa vs 150 kDa), ii) a low risk of cytotoxicity, iii) easy conjugation thanks to the three
109 internal disulfides, and iv) good stability at physiological conditions and neutral pH (Grapa *et al.*, 2019;
110 Silva *et al.*, 2016). Many studies have confirmed the benefits of EGF-conjugated NPs in increasing the
111 cell uptake and in the tumor accumulation that yield better anti-tumor activities and reduced
112 systemic toxicity.

113 Venugopal *et al* carried out a standard example for EGF-conjugated NPs. The authors showed that by
114 conjugating EGFs onto their co-polymeric PLGA-PEG NPs, a significant reduction of breast cancer cells
115 (MDA-MB-468) viability (around 10.6 %) and a 93-fold higher paclitaxel accumulation had been
116 achieved in the corresponding tumor group compared to the group treated with non-targeted NPs
117 (Venugopal *et al.*, 2018). In another effort to improve the radiotherapy efficiency in esophageal
118 cancer, Gill *et al* constructed PLGA NPs functionalized with EGF proteins for a specific delivery of a

119 therapeutic radionuclide. The finalized NPs presented a better cellular uptake and a greater
120 radiotoxicity in EGFR-overexpressed cancer cells (OE21) compared to normally EGFR-expressed
121 cancer cells or healthy cells. This specific delivery reduced significantly the toxicity of the
122 encapsulated radionuclide on healthy cells and might lead to fewer side effects for further clinical
123 applications (Gill *et al.*, 2018).

124 In addition to targeting properties, when an EGF protein is introduced to highly charged NPs such as
125 dendrimers, it neutralizes the highly positive charges of these NPs and may minimize their toxicity.
126 This phenomenon was observed in the study of Li *et al.* In fact, by conjugating EGF protein onto
127 positive dendrimers for a better gene delivery, the authors were successful to not only enhance the
128 *in vivo* EGFR-positive breast cancer (MDA-MB231) tumor accumulation of the EGF-dendriplexes but
129 also decrease the cytotoxicity of dendrimers compared to conventional dendrimers (Li *et al.*, 2015a).

130 All the aforementioned studies have demonstrated the attractive potency of EGF proteins as EGFR
131 active targeting ligand in cancers. Nevertheless, its clinical application remains challenged by several
132 issues. On one side, murine EGF proteins are prone to immunogenicity problems. On the other side,
133 EGF proteins from human sources or recombinant ones are relatively complex and expensive, that
134 may explain why its application is limited to the laboratory scale.

135 **2.1.2. Anti-EGFR affibodies**

136 Affibodies (Afbs) are scaffold proteins with a 3-helix bundle structure and are composed of 58 amino
137 acids. Anti-EGFR affibodies (Table 2) are engineered to have i) high affinity and specificity to EGFRs
138 with a K_d around 2.8 nM, ii) a low molecular weight and size (7 kD and 1-2 nm), iii) high stability and
139 easy conjugation via its terminal cysteine, iv) lower immunogenicity than traditional antibodies
140 (Jokerst *et al.*, 2011; Lucky *et al.*, 2016; Yoo *et al.*, 2019; Y. Zhang *et al.*, 2018).

141 The presence of anti-EGFR affibodies on the surface can help NPs better internalize (faster and higher)
142 into EGFR-positive cancer cells, deliver drug more efficiently into tumor sites (higher concentration
143 and longer retention), and attenuate cytotoxicity on normal cells. As an example, Lucky and co-
144 workers functionalized their upconversion NPs with an anti-EGFR affibody for a better photodynamic
145 therapy (PDT) against oral cancer. The affibody-decorated NPs internalized more rapidly and
146 efficiently in EGFR-overexpressed oral cancer cells (OSCC cells) than non-targeted NPs (3.8 folds), or
147 low EGFR expressing cancer cells (MCF-7 and HepG2 cells). Thanks to this specificity, higher PDT
148 toxicity in EGFR positive cells (A431 and OSCC cells) than EGFR negative MCF-7 cells (35 % vs 0 %
149 respectively) was achieved. Furthermore, this study also pointed out that the interaction between
150 the grafted anti-EGFR affibodies on the NPs and the cell-surface EGFRs was a prerequisite for an
151 enhancement in the cellular uptake (Lucky *et al.*, 2016). Kwon *et al* developed protein/gold core/shell
152 NPs for targeted and nanotoxicity-free cancer therapy. To be precise, the core of these NPs was
153 made of hepatitis B virus capsids decorated with anti-EGFR affibodies for active targeting and dotted
154 with many small gold NPs for the photothermal activity (PTT). The affibodies present on the surface
155 helped the targeted NPs to be effectively delivered to EGFR-overexpressed breast cancer cells (MDA-
156 MB-468) and increased the tumor cell necrosis with a remarkable tumor size reduction compared to
157 the bare AuNPs. In addition, the affibody-free AuNPs caused extensive and histological damages to
158 the liver and the kidney, whereas no visible macroscopic and histological change was observed in
159 major organs for three weeks post-injection in the case of targeted NPs (Kwon *et al.*, 2014).

160 **2.1.3. Anti-EGFR repebodies**

161 Anti-EGFR repebodies are another kind of protein that can be applied in EGFR active targeting with
162 nanomedicines. Repebodies are a scaffold protein composed of leucine-rich repeated modules. In

163 addition to a relatively good binding affinity towards EGFRs ($K_d= 9.18$ nM), simple engineering and
164 good specificity, these non-antibody proteins possess a smaller molecular size (30 kDa) and present
165 better tissue penetration compared to entire antibodies (Table 2). For the production, anti-EGFR
166 reprobodies can be cloned into a pET21a vector with polyhistidine and polyanionic tags at the N-
167 terminal and C-terminal ends. The constructed vector is then transformed into an *E. coli* host strain
168 (Pyo *et al.*, 2018).

169 Due to its EGFR-binding ability, anti-EGFR reprobodies were conjugated onto NPs in several studies for
170 better targeting EGFR-positive tumors. For instance, Lee and co-workers fused an anti-EGFR
171 reprobody to apoptin, which is a tumor-selective apoptotic protein for cancer treatment. The
172 resulting amphiphilic monomers could be self-assembled into micelles with a size around 48 nm, a
173 high homogeneity and stability level. Consequently, the cellular uptake of the targeted NPs increased
174 significantly according to the EGFR expression level of the cancer cells, which confirmed the targeting
175 activity of the ligand. In addition, the cytotoxicity of the EGFR positive cancer cells (A431 and MDA-
176 MB-468 cells) treated with the targeted NPs was remarkably enhanced compared to the negligible
177 apoptotic activity of the free protein, or modest cytotoxicity against H1650 cells expressing a
178 moderate level of EGFR, or low cytotoxicity against EGFR low-expressing cells (MCF-7) (Lee *et al.*,
179 2017).

180 Similar to the role of EGF protein in targeted nanomedicines with dendrimers, anti-EGFR reprobodies
181 once conjugated to highly charged NPs, can both help increase the drug delivery efficiency and
182 attenuate the cytotoxicity linked to high charges. Using this strategy, Kim and colleagues fused
183 genetically a polyanionic peptide to their anti-EGFR reprobody that allowed its further conjugation
184 with positively charged dendrimers. As expected, the gene delivery efficiency of the targeted
185 dendrimers was correlated with the EGFR expression level due to the ligand targeting properties. In
186 addition, the toxicity of the targeted dendrimers decreased with an increase in the reprobody's
187 amount on the NPs. This result indicated the perspective of using active targeting ligands to
188 overcome the limitations of toxicity in dendrimers' application (Kim *et al.*, 2018).

189 Both anti-EGFR affibodies and reprobodies belong to the group of non-antibody scaffolds and appear
190 as interesting alternatives to conventional antibodies in EGFR targeting with nanomedicines. As
191 therapeutic agents, the small size of these proteins may pose a major disadvantage in terms of short
192 plasma half-life time (Gebauer and Skerra, 2020; Vazquez-Lombardi *et al.*, 2015), but in the case of
193 nanomedicines functionalized with targeting moieties, the half-life time of the finalized NPs depends
194 mainly on the properties of nanocarriers. Nevertheless, if the blood circulating time of the resulting
195 NPs is not sufficient to have efficient therapeutic activities, one of the roots may come from these
196 fragments. Therefore, several methodologies may be applied on targeting ligands to improve the
197 stealthiness of the finalized NPs such as Fc fusion or polyethylene glycol (PEG) conjugation.

198 **2.2. Anti-EGFR whole antibodies**

199 Monoclonal antibodies (mAbs) are largely recognized as the most popular targeting ligand in the field
200 of nanomedicines due to their safety; high tendency and specificity to target receptors (Alibakhshi *et*
201 *al.*, 2017a).

202 They are Y-shaped proteins made of four polypeptide subunits and composed of identical heavy and
203 light chains. Their arms are termed "fragment antigen-binding domains" (Fab) and the tail is termed
204 "fragment crystallization domain" (Fc) with the role of activating cascades (Table 2). Each heavy chain
205 and each light chain are composed of heavy and light variables (VH, VL), which create the site-binding
206 region and constant (CH, CL) regions (Alibakhshi *et al.*, 2017a).

207 After binding to target receptors expressed at the cell surface, mAbs can cause a direct cytotoxic
208 effect by inducing the apoptosis or block the corresponding ligands/cognate receptors. For tumor
209 cells, as soon as mAbs interact with their receptors, the Fc domain can trigger cell destruction by the
210 engagement of host immune effector mechanisms. This process includes two main pathways: i) the
211 activation of cytotoxic enzymes of the complement cascade and/or ii) the triggering of cytotoxic
212 effects of innate immune cells such as natural killer cells via the activation of Fc receptors or the
213 phagocytosis activation by monocytes/macrophages (Marabelle and Gray, 2015).

214 For the EGFR-targeting, a number of human mAbs have been developed such as cetuximab;
215 necitumumab; matuzumab; nimotuzumab and panitumumab (Li *et al.*, 2015b; Maya *et al.*, 2013).
216 Among these mAbs, cetuximab (Cet; C225 or Erbitux®) is the most widely used in cancer treatment
217 both as a therapeutic agent and as an active targeting ligand (Maya *et al.*, 2013). Cetuximab is the
218 first FDA-approved EGFR-specific mAb for the treatment of EGFR-expressing metastatic colorectal
219 cancer in combination with FOLFIRI (irinotecan, 5-fluorouracil, and leucovorin) (Li *et al.*, 2016). It is
220 also indicated for the treatment of the locally advanced squamous cell carcinoma of the head and
221 neck in combination with radiation therapy and for the recurrent or metastatic squamous cell
222 carcinoma. This mAb is a chimeric human antibody (MW = 145.78 kD) from the immunoglobulin IgG1
223 class that specifically targets the human EGFR with a higher binding affinity ($K_d = 0.39$ nM) than EGFR
224 natural ligands such as EGF protein or the transforming growth factor- α . Cet blocks ligand-binding
225 and inhibits ligand-induced phosphorylation and activation of the EGFR tyrosine kinase. C225 has
226 been shown to be effective in several antitumor processes including the G0/G1 cell-cycle arrest, the
227 induction of apoptosis, the inhibition of DNA repair, the anti-angiogenesis, the tumor cell motility,
228 invasion, and metastasis. However, the application of Cet remains challenged by potential cytotoxic
229 effects through antibody-dependent cell-mediated cytotoxicity (Baselga, 2001; Specenier and
230 Vermorken, 2013).

231 Numerous studies proved that the functionalization of NPs with Cet can enhance effectively drug
232 cellular internalization into EGFR-overexpressed cancer cells. Furthermore, Cet-modified
233 nanoparticles are able to recognize specifically EGFR-overexpressing cells and present better
234 therapeutic and diagnostic effects with less toxicity on normal cells (Chu *et al.*, 2015; Costa *et al.*,
235 2017). Up to now, Cet remains the most used active targeting ligand in EGFR targeted nanomedicines.
236 Liu *et al* developed a multifunctional Cet-conjugated liposomal system encapsulating doxorubicin,
237 AuNPs and SPIONs for theranostic application. Efficient Cet-mediated targeting with a higher cellular
238 uptake of NPs in the EGFR-overexpressed skin cancer (A431 cells) was achieved for the targeted NPs
239 compared to the free drug or the non-targeted NPs. This better cellular uptake not only increased
240 the cytotoxicity of drug towards cancer cells but also improved the PDT activity of its metallic
241 component. *In vivo*, the MR and optical imaging reconfirmed the specific tumor targeting of the
242 targeted NPs with a clear tumor accumulation and its promotion on the tumor destruction. Finally,
243 without major morphological damages to normal tissues, these targeted NPs clearly demonstrated
244 the benefit of having Cet on the surface and presented their potency as a theranostic tool for cancer
245 treatment (Liu *et al.*, 2019). In another study, Yoon and co-workers conjugated Cet onto their
246 PEGylated dendrimers for better gene delivery. The authors were successful in delivering more
247 efficiently oncolytic adenovirus into EGFR-positive tumors with the targeted dendrimers than the
248 non-targeted dendrimers or the naked gene. In EGFR positive cancer cells (A549 cells), the targeted
249 dendrimers with Cet showed an 8.6-fold and a 6.5-fold higher gene cellular uptake than the naked
250 gene or the Cet-free dendrimers, respectively. Furthermore, the immunogenicity and hepatotoxicity
251 linked to the highly charged dendrimers were also significantly attenuated thanks to the charge
252 neutralization of Cet (Yoon *et al.*, 2016).

253 Besides the benefit as an active targeting ligand, conjugated Cetuximab on NPs can also present its
254 therapeutic potency. Qian *et al* reported that the conjugation of Cet on AuNPs enhanced the
255 cytotoxicity of Cet in non-small lung cancer (NSCLC) compared to the free Cet. Indeed, the
256 therapeutic effect of Cet-decorated AuNPs was more pronounced in EGFR-overexpressed A459 cells
257 compared to low EGFR-expressed H1299 cells that reflected a selective targeting of Cetuximab.
258 Furthermore, due to the enhancement in EGFR endocytosis and the subsequent suppression of the
259 downstream signaling pathway, the apoptotic activity of Cet-AuNPs was significantly higher than that
260 of free Cet, as reflected by a higher reduction in tumor weight and volume with a lower toxicity level
261 (Qian *et al.*, 2015). This discovery suggested a new strategy to use multifunctional ligands as both
262 active targeting and therapeutic agents in nanomedicines.

263 In addition to cetuximab, other human mAbs such as panitumumab (Vectibix®) and nimotuzumab (h-
264 R3) may also be used for nanoconjugation (Li *et al.*, 2015b; Yook *et al.*, 2015). Panitumumab is a fully
265 humanized mAb belonging to the class IgG2a and clinically used to inhibit metastatic colorectal
266 cancer in combination with chemotherapy (Lin *et al.*, 2018; Yook *et al.*, 2015). This IgG2 mAb exhibits
267 an approximate 8-fold greater binding affinity than cetuximab (K_d around 0.05 nM) and contains no
268 murine protein sequences that may reduce the risk of hypersensitive reactions. In clinical
269 applications, the anti-tumor activity and toxicity of panitumumab was similar to that of cetuximab
270 despite its higher binding affinity (Kim and Grothey, 2008). This observation may call into question
271 the necessity of using ligands with a super-high affinity. Similar to that of Cetuximab, the conjugation
272 of panitumumab onto NPs also presented several benefits such as selective drug delivery into EGFR
273 positive tumors. As an example, Yook *et al* constructed a novel radiation nanomedicine for the
274 treatment of EGFR positive breast cancer by modifying its AuNPs with panitumumab. By comparing
275 the cell-bound radioactivity of the antibody-conjugated NPs and the bare NPs, the authors
276 demonstrated the specific binding of the targeted NPs to EGFR positive cancer cells and this binding
277 was found to be dependent to their EGFR density. In fact, this value was 3.1 times and 22.1 times
278 greater in MDA-MB-468 cells than in MDA-MB-231 and MCF-7 cells with high, moderate and low
279 EGFR density respectively. At the same dose of radioactivity, the survival rate of MDA-MB-468 cells
280 treated with targeted NPs was clearly low compared to that of MDA-MB-231 cells or MCF-7 cells
281 (0.001 % vs 33.8 % and 25.8 %). Compared to the non-targeted NPs, the radiotoxicity of the targeted
282 NPs towards MDA-MB-468 cells was also significantly greater (0.001 % vs 8.4 %) (Yook *et al.*, 2015).

283 Nimotuzumab (h-R3) is a humanized IgG1 isotype mAb that binds to the extracellular domain of the
284 EGFR and inhibits the EGFR-ligand binding. This mAb has been approved for the treatment of head
285 and neck tumors, and is in clinical trials for other kinds of cancers with a high-level expression of
286 EGFR. Compared to cetuximab, h-R3 shows a lower binding affinity towards EGFRs in human cells
287 with a K_d around 4.53 nM. Nevertheless, one of the biggest advantages of nimotuzumab compared to
288 Cet or panitumumab is the absence of severe adverse effects such as skin, renal, and gastrointestinal
289 mucosa toxicities (Li *et al.*, 2015b; Ramakrishnan *et al.*, 2009). In EGFR-targeting nanomedicines, NPs
290 functionalized with nimotuzumab exhibited satisfactory results in terms of cellular uptakes and
291 tumor accumulation. As an example, in an attempt to better deliver gene into EGFR-overexpressed
292 cancer cells, Li and colleagues decided to introduce h-R3 onto their dendrimers. The decoration of h-
293 R3 on dendrimers helped enhance the gene transfection efficiency with higher nuclear accumulation
294 in the EGFR positive HepG2 cells compared to the free-antibody dendrimers. On the other hand, the
295 innate cytotoxicity of dendrimers due to their high charges was significantly decreased due to the
296 neutralizing effect of h-R3 (Ramakrishnan *et al.*, 2009). All these results demonstrated that
297 panitumumab or nimotuzumab could be used as alternative to Cetuximab in EGFR-targeted
298 nanomedicines.

299 **2.3. Anti-EGFR antibody fragments**

300 Although the presence of mAbs on NPs presents undeniable benefits, antibody-functionalized NPs
301 also encounter several restrictions including i) poor stability due to the antibody large size (MW=150
302 kDa) (Richards *et al.*, 2017), ii) high immunogenicity (Byrne *et al.*, 2008; Richards *et al.*, 2017), iii)
303 rapid elimination (Ashton *et al.*, 2018; Richards *et al.*, 2017), and iv) the lack of conjugation specificity
304 that may hinder ligand-receptor binding (Byrne *et al.*, 2008). To overcome these issues and thanks to
305 insight knowledge in the antibody structure, researchers are able to disassemble an antibody into
306 fragments in accordance with specific purposes such as: Fab, Fab', F(ab')₂ and Fv regions. In addition,
307 with the help of protein engineering, a novel class of antibody fragments has been constructed and
308 can serve as alternatives to conventional mAbs. In the case of EGFR-targeting, several antibody
309 fragments of this novel class have been engineered and applied in nanomedicines including Fabs,
310 scFvs, nanobodies, and bispecific antibodies (Alibakhshi *et al.*, 2017b; Richards *et al.*, 2017). All these
311 antibody fragments preserve the specificity of an antibody by retaining at least one antigen-binding
312 region. Therefore, once these fragments are conjugated to NPs, the active targeting is preserved or
313 even better than the original mAbs. Numerous advantages for the functionalization of NPs with these
314 fragments compared to the whole mAbs have been revealed such as better conjugation of targeting
315 ligands and attenuated immunogenicity. In fact, as these fragments are devoid of an Fc effector
316 region and 100 % humanized, the complement activation might be avoided and the risk of
317 hypersensitive reactions are reduced (Byrne *et al.*, 2008). In addition to less immunogenicity, the
318 smaller size of these fragments leads to higher loading capacities and a superior orientation of
319 conjugated ligands on the NPs. This property may result in an overall enhancement in conjugation
320 efficacy (Byrne *et al.*, 2008; Richards *et al.*, 2017).

321 **2.3.1. Anti-EGFR Fab fragments**

322 In the field of medicine, antigen-binding fragments (Fabs) are considered the conventional form of
323 antibody fragments and were first introduced in 1995 (Alibakhshi *et al.*, 2017a; Nelson, 2010). Fabs
324 can be produced by disassembling an intact mAb into two Fabs of 50 kDa using the protease papain or
325 via artificial engineering. A Fab is composed of one VH and one VL chain linked together by disulfide
326 bonds and contains a single antigen-binding site (Alibakhshi *et al.*, 2017a). In comparison to full
327 antibodies, Fab fragments are less immunogenic and smaller (MW = 50 kDa). The smaller size of Fabs
328 may allow a higher density, a better orientation of conjugated ligands on NPs, and can cause less
329 perturbation to the NPs physicochemical properties (**Table 2**) (Houdaihed *et al.*, 2020). Once Fabs are
330 conjugated to NPs, their presence has been proved to provide higher cellular internalization and
331 improved the therapeutic efficacy in many studies.

332 As an example, Zhai *et al* conjugated an anti-EGFR Fab with a K_d at 5.6 nM onto their lipid NPs.
333 Consequently, a higher specificity towards EGFRs was achieved with the targeted NPs compared to
334 the bare NPs (Zhai *et al.*, 2015). In another study, Houdaihed and co-workers combined the EGFR and
335 HER2 targeting by decorating their polymeric NPs with anti-HER2 and anti-EGFR Fab fragments to co-
336 deliver three therapeutic agents into EGFR positive breast cancer tumors. In fact, trastuzumab and
337 panitumumab antibodies were digested using protease papain to produce anti-HER2 and anti-EGFR
338 Fab fragments, respectively. These fragments were then conjugated onto PEG-PLGA NPs using the
339 covalent method. As a result, a better cellular uptake due to Fab fragments was confirmed by a
340 clearly higher cytotoxicity of the dual-targeted NPs than the HER2 mono-targeted and the non-
341 targeted NPs in HER2-EGFR overexpressed cells (SK-BR-3). On the contrary, no significant difference
342 in cytotoxicity was observed in HER2-EGFR negative cells (MCF-7) treated with these three types of
343 NPs. This study not only demonstrated the benefit of using anti-EGFR Fab fragments as active

344 targeting ligands but also suggested that the dual-targeting strategy may help to better deliver drug
345 into tumors with the heterogeneity of receptor expression (Houdaihed *et al.*, 2020).

346 **2.3.2. Single chain antibody fragments**

347 Single chain antibody fragments or scFv are the second type of antibody fragments used as active
348 targeting ligands in nanomedicines. It is made of a single polypeptide chain with the size of 25 kDa. In
349 their structure, these antibody fragments (Table 2) have a monovalent structure with a good affinity
350 for a single antigen and comprises a heavy chain and a light chain linked together via a short flexible
351 peptide linker. The glycine and serine residues in the linker sequence make the scFv flexible and
352 resistant to protease (Ahmad *et al.*, 2012; Alibakhshi *et al.*, 2017a). In order to generate high-affinity
353 and high-specificity scFv fragments, new selection and display technologies such as phage display or
354 ribosome display are available to isolate scFv with desirable properties (Alibakhshi *et al.*, 2017a;
355 Holliger and Hudson, 2005).

356 As an example for EGFR-targeting with scFv in nanomedicines, Yang and colleagues used an anti-
357 EGFR with a good binding affinity ($K_d=3.36$ nM) to functionalize their quantum dots (QD) and
358 superparamagnetic iron oxides nanoparticles (SPIONs) for breast cancer and pancreatic tumor *in vivo*
359 imaging. The results showed that both the targeted QD and SPIONs with anti-EGFR scFv specifically
360 bound and better internalized into EGFR-expressing breast cancer (MDA-MB-231 and 4T1) and
361 pancreatic cancer (MIA Paca-2) cells. As a result, these targeted NPs provided a significantly better
362 fluorescent signal and contrast for the fluorescence and MR imaging compared to their counterparts
363 (Yang *et al.*, 2009). In our team, NPs functionalized with anti-EGFR scFv also draw a great interest. We
364 developed a novel nanomedicine based on the complexation between a humanized anti-EGFR scFv-
365 SPION, siRNA and cationic polymers for a better gene delivery into triple negative breast cancer cell
366 (MDA-MB-231). Our study pointed out that a better cellular uptake could be achieved thanks to the
367 presence of anti-EGFR scFv and the cellular uptake can be increased with an increase in the scFv
368 amount on NPs. As a result, this better cancer cellular uptake led to better gene silencing effects
369 compared to the non-targeted NPs (69.4 % vs 25.3 %) (Vinh Nguyen *et al.*, 2020). All the above
370 results have demonstrated the promising application of NPs decorated with anti-EGFR scFv in the
371 enhancement of NPs' therapeutic efficiency.

372 **2.3.3. Anti-EGFR nanobodies**

373 Nanobodies (Nbs) or VHH single-domain antibodies are the next type of EGFR-antibody fragments
374 used in nanomedicines. This kind of fragment (Table 2) is an antigen-binding fragment of camelid and
375 shark heavy-chain antibodies (HcAbs) with dimensions in the nanometer range (Muyldermans, 2013).
376 Compared to the traditional mAbs, nanobodies offer several advantages including i) a small size (4
377 nm long and 2.5 nm wide) and a low molecular weight (15 kDa) that facilitate tumor accumulation
378 and offer a higher density of ligands on the NPs surface, ii) thermal and chemical resistance that
379 permits its use in hard conditions, iii) high solubility and stability allowing an easier conjugation onto
380 nanoparticles, iv) high specificity and binding affinity, and v) low immunogenic potential due to the
381 lack of Fc components (Alibakhshi *et al.*, 2017a; Altintas *et al.*, 2013; Kooijmans *et al.*, 2016;
382 Muyldermans, 2013; Wang *et al.*, 2017). Moreover, the production of nanobodies is easier than that
383 of conventional mAbs, which refers to a multi-stage process with several steps including i) the
384 immunization of camels or lama with the target antigen, ii) the cloning of the V gene repertoire from
385 peripheral blood lymphocytes and iii) the selection of target-specific Nbs through phage display
386 (Alibakhshi *et al.*, 2017a).

387 In targeting nanomedicines, the anti-EGFR nanobodies have been engineered and are getting
388 increasing attention. Roovers *et al* succeeded to produce anti-EGFR nanobodies with good binding

389 affinities (K_d from 5 to 20 nM) that may be used for further functionalization in NPs. These
390 nanobodies potently inhibited EGF-dependent cell proliferation and their antitumor activity was
391 found to be similar to that of Cetuximab (Roovers *et al.*, 2011). Altintas and co-workers constructed
392 novel EGFR targeting nanobody-functionalized albumin NPs to deliver a multikinase inhibitor to EGFR
393 overexpressing tumor cells. Compared to non-targeted NPs, nanobody-conjugated NPs exhibited a
394 40-fold higher binding affinity to EGFR-positive 14C squamous head and neck cancer cells. Therefore,
395 the targeted NPs led to a successful release of drug in cancer cells and inhibited cell proliferation,
396 whereas the non-targeted formulation showed no anti-proliferative activity on cancer cells (Altintas
397 *et al.*, 2013). In another study, Wang *et al.* developed quantum-dot based polymeric micelles
398 conjugated with an anti-EGFR nanobody and encapsulating aminoflavone for EGFR-overexpressing
399 MDA-MB-468 triple-negative breast cancer theranostics. Due to the enhancement and selectivity in
400 the cellular uptake compared to the non-targeted NPs (67-fold), the targeted NPs offered a better
401 fluorescence signal for *in vivo* NPs biodistribution studies. Furthermore, aminoflavone encapsulated
402 in the targeted NPs was found to better accumulate in tumor sites and exhibited a more effective
403 tumor inhibition without observable systemic toxicity (Wang *et al.*, 2017). All above studies revealed
404 remarkable advantages of using anti-EGFR nanobodies as active targeting ligands in nanomedicines,
405 especially in terms of tumor penetration ability. In this aspect, the nanobody-decorated NPs are one
406 of the most effective nanocarriers in the frame of this review.

407 **2.3.4. Anti-EGFR bispecific antibodies**

408 Due to the contribution of multiple factors in cancer and the blockage of several targets that might
409 result in better efficacy, the concept of bispecific antibodies (BsAb) for dual-targeting appears as a
410 potential strategy for better targeting with NPs (Krishnamurthy and Jimeno, 2018). A BsAb (Table 2)
411 is made of two different antibodies or antibody derivatives (such as scFv, Fab, etc.) that allows a
412 simultaneous recognition of two different receptors (Alibakhshi *et al.*, 2017a). BsAb was initially
413 produced by the reduction and re-oxidation of hinge cysteines in mAb or through the fusion of two
414 hybridoma cell lines. Recently, the development of recombinant DNA technology helps to facilitate
415 the BsAb production with a greater variety (Krishnamurthy and Jimeno, 2018). In comparison to
416 conventional antibodies, several advantages can be achieved with BsAb such as: i) an enhancement
417 in tumor killing by redirecting cytotoxic T and natural killer (NK) cells, ii) the retargeting of toxins,
418 radionuclides or cytotoxic agents, iii) the blockage of two different mediators or pathways, iv) an
419 increase in binding specificity via interactions with two different receptors (Alibakhshi *et al.*, 2017a).

420 A standard example of the BsAb application in EGFR targeting NPs was performed in the study of Wu
421 *et al.* The authors developed a bispecific antibody conjugated to SPIONs for the targeted MR imaging
422 in both HER2 and EGFR-overexpressing tumors. The bispecific antibody was created by linking an
423 anti-EGFR scFv to an anti-HER2 scFv via a flexible peptide linker. The binding affinity (K_d) of the
424 resulting BsAb was determined to be 10 and 3 nM towards EGFR and HER2 protein respectively, and
425 was comparable to that of the corresponding scFv. Compared to the non-targeted NPs, the dual-
426 targeted SPIONs exhibited their targeting properties both for EGFR and HER2 receptors. In fact,
427 compared to the non-targeted NPs, a better targeting activity was achieved for the dual-targeted NPs
428 incubated with HER2+/EGFR+ cancer cells (SK-BR-3) and HER2+/EGFR++ cancer cells (A431). On the
429 contrary, both the dual-targeted NPs and the non-targeted NPs binds poorly to HER2-/EGFR-
430 cancer cells (Colo-205). Moreover, this specific targeting ability was clearly pronounced in SK-BR-3
431 cells compared to Colo-205 cells by a factor of 61.5 greater in the contrast enhancement at 24 hours
432 post-injection. As a result, the contrast of MR imaging in HER2-EGFR positive tumors (SKBR-3 and
433 A431 cells) was obviously enhanced 94.8 and 84.1 %, respectively (Wu *et al.*, 2016).

434 Besides the dual-targeting application to increase the drug delivery efficiency, bispecific antibodies
435 can also facilitate the conjugation of active targeting ligands onto the NPs surface. This strategy relies
436 on the use of BsAb that, one side, can recognize the target receptor on the cell surface, and on the
437 other side, can bind to a component of NPs such as their polymer layer. Using this strategy, Cui and
438 colleagues developed a bispecific antibody targeting polyethylene glycol (PEG) and EGFRs by
439 connecting two corresponding scFv specificities via a glycine-serine linker (G4S). The bispecific
440 antibody was able to bind to the PEGylated NPs and allowed the conjugation of anti-EGFR ligands
441 onto the PEGylated NPs without any modification on anti-EGFR ligands. *In vitro*, the resulting NPs
442 exhibited an enhancement in the targeting and internalization into triple-negative breast cancer cells
443 overexpressing EGFRs (MDA-MB-468) compared to their PEGylated counterparts. This result
444 confirmed the EGFR targeting activity of the anti-EGFR scFv in this bispecific antibody and
445 demonstrated the perspective of this conjugation method. However, there was no difference in
446 tumor accumulation for the targeted and the non-targeted NPs *in vivo*. The authors claimed that the
447 BsAb functionalization might influence the stealthiness of the NPs in *in vivo* environment with
448 complicated conditions (Cui *et al.*, 2019). Although there are still steps to optimize, this study
449 highlighted the perspective of using BsAb in NPs functionalization when physical and chemical
450 methods are not suitable.

451 The application of antibody fragments have shown a great interest in EGFR targeting with
452 nanomedicines for both, therapeutic and diagnostic applications in cancer therapy. These antibody-
453 based fragments not only help to address the issues that normally we confront with traditional mAbs
454 but also offer unique milestones, especially in terms of tumor penetration and double or even
455 multiple targeting. However, similar to scaffold proteins, the quick clearance is one of the biggest
456 limitations for the use of antibody fragments in *in vivo* level and needs to be carefully considered in
457 design steps. Besides, while antibody-based strategies have proven their potency in clinical
458 applications for cancer treatment for long time, the use of these fragments are relatively new.
459 Therefore, their safety must be evaluated in deep.

460 **2.4. GE11 peptide**

461 Recently, peptides have emerged as one of the most promising alternatives to antibodies and their
462 derivatives have been used as active targeting ligands in nanomedicines. In comparison with
463 conventional mAbs, several advantages can be enlisted for peptides including i) lower
464 immunogenicity, ii) good penetration into tumors, iii) easy synthesis, and iv) better conjugation (Pi
465 *et al.*, 2017). To achieve good targeting properties, the selection of appropriate peptides for each kind
466 of receptors plays a key role. Nowadays, the screening of phage display libraries is normally used to
467 select ligands for a specific receptor (Li *et al.*, 2005).

468 Among available peptides for EGFR-targeting, the GE11 peptide (Table 2) is the most widely exploited
469 as active targeting agent in EGFR-targeting nanomedicines. GE11 is a small peptide of 12 amino acids
470 (MW = 1540 g/mol) whose sequence is NH₂-Y-H-W-Y-G-Y-T-P-Q-N-V-I-CO₂H. In terms of EGFR binding
471 affinity, the GE11 peptide bind specifically and efficiently to one EGFR region with a K_d ~22 nM (Li
472 *et al.*, 2005). This peptide has a relatively lower affinity than EGF protein (K_d = 2 nM) or mAbs. However,
473 it is much smaller, does not have any mitogen activity and manifests less immunogenicity.
474 Furthermore, GE11 can be easily produced by microwave-assisted solid phase automated synthesis
475 (Pi *et al.*, 2017).

476 Recent studies have revealed that GE11 is able to accelerate the cellular uptake of NPs via the EGFR-
477 dependent endocytosis. This enhancement in internalization helps improve tumor inhibition effects
478 and significantly reduce the NPs toxicity against normal cells (Pi *et al.*, 2017). GE11-decorated NPs

479 provide a new strategy for cancer treatment with higher therapeutic efficacy and fewer side effects.
480 As an example, Milane and co-workers introduced GE11 onto their polymeric NPs to co-deliver
481 paclitaxel and lonidamine for the treatment of multidrug-resistant in breast and ovarian tumors. The
482 authors investigated the intracellular internalization pathway of the targeted and non-targeted NPs
483 and showed that the targeted NPs entered the EGFR positive cancer cells (OVCAR5, SK-OV-3-TR and
484 MDA-MB-231 cells) and through the EGFR-mediated pathway, whereas the non-targeted NPs
485 internalized via the non-specific endocytosis. In addition, the GE11-NPs exhibited a greater cellular
486 uptake with an increasing EGFR expression level and a superior pharmacokinetic profile than the free
487 drug and the GE11-free NPs. Finally, in EGFR positive multidrug-resistant ovarian and breast cancer
488 cells (hypoxic and normoxic SK-OV-3 and MDA-MB-231 cells, respectively), the targeted NPs
489 exhibited very interesting anti-tumor activities by causing the cell death up to 90-95 %. This study
490 showed that the targeted NPs with the GE11 peptide may be a good solution to overcome the
491 problem of the multi-drug resistance in EGFR-overexpressing cancers (Milane *et al.*, 2011).

492 Thanks to its smaller size than other kinds of ligands, GE11 occupies smaller space on the NPs surface
493 and facilitates other ligands' introduction that might help target better tumors and minimize off-
494 target effects. Using this strategy, Talekar and colleagues designed a dual CD44/EGFR targeting NPs
495 to deliver miRNA into lung cancer cells (SK-LU-1). In comparison with the single CD44-targeted NPs,
496 the dual-targeted NPs showed a 20-fold increase in the expression of loaded miRNA in the target
497 cells. *In vivo*, when the single CD44-targeted NPs exhibited a 7-fold increase in the miRNA expression
498 than the non-targeted NPs, an increase by a factor of 12 in the gene expression was obtained for the
499 dual-targeted NPs (Talekar *et al.*, 2016).

500 Another benefit of GE11 is the possibility for it to be introduced onto amphiphilic molecules that can
501 later self-assemble into micelles with good drug loading capacity. Using this strategy, to co-deliver
502 gemcitabine and olaparib for the treatment of pancreatic cancer with breast cancer 2-mutation, Du
503 *et al* introduced GE11 on the hydrophilic domain of an amphiphilic molecule that self-assembled into
504 micelles. The targeted micelles presented better tumor targeting in EGFR-overexpressed pancreatic
505 cancer cells (Capan-1) than the non-targeted micelles. On the other hand, the extensive
506 internalization of the targeted NPs in EGFR positive pancreatic cancer Capan-1 cells compared to
507 other cell lines (primary human pancreatic stellate H-PSC cells and human umbilical vein endothelial
508 HUVEC cells) with a lower EGFR level highlighted the EGFR targeting activity of the conjugated GE11.
509 As expected, a clear enhancement of antitumor effects was obtained for the targeted NPs among all
510 the treatment groups with the non-targeted NPs or the free drug (Du *et al.*, 2018).

511 Interestingly, Biscaglia and co-workers investigated the benefit of using GE11 as a targeting ligand
512 compared to Cetuximab. In this study, the authors introduced GE11 or Cet onto their AuNPs and
513 compared their EGFR targeting activity *in vitro*. The GE11-AuNPs on one side exhibited better
514 targeting towards EGFR positive cancer cells (Caco-2 and SW480) compared to EGFR negative cells
515 (SW620). Besides, despite its lower binding affinity, GE11-AuNPs achieved a better targeting activity
516 than Cet-NPs in EGFR-overexpressed cells. To explain this phenomenon, the authors proposed that
517 the organization of GE11 on the surface of nanosystem was more favorable for its interaction with
518 EGFRs on the cell surface and resulted in a better active targeting activity. Although these results are
519 limited to AuNPs and needed more studies, especially *in vivo* ones, to confirm, this study pointed out
520 the importance of controlling the organization of conjugated ligands for an efficient targeting activity
521 (Biscaglia *et al.*, 2017).

522 All previous studies indicate that GE11 is a useful targeting ligand for EGFR targeting with the help of
523 nanomedicines. Compared to other kinds of EGFR ligands, GE11 is outstanding regarding its ease in
524 conjugation to nanocarriers, which makes it suitable to most kinds of nanoparticles and conjugation

525 strategies. However, as GE11 binding affinity is relatively lower than other kinds of EGFR targeting
526 ligands, its density on NPs plays an essential role in the targeting properties of the finalized NPs, and
527 extensively depends on the conjugation methods. Therefore, one of the most important parameters
528 to be carefully considered during the development of targeting nanomedicines with GE11 is the
529 selection of appropriate conjugation strategies. To this end, the conjugation method should be
530 selected according to each kind of NPs and GE11 density needs to be controlled after the conjugation
531 to ensure that the resulted NPs possess an efficient targeting activity for EGFR.

532 2.5. Anti-EGFR aptamers

533 In addition to peptides, aptamers are another alternative to protein ligands. Aptamers are
534 considered “chemical antibodies” due to their functional similarity and the possibility to recognize
535 their target with high specificity and affinity. Furthermore, while traditional mAbs are highly
536 immunogenic, expensive and difficult to synthesize, aptamers provide remarkable advantages over
537 protein antibodies, both in synthesis and application including i) a smaller molecular weight (8-25
538 kDa), ii) better and faster tissue penetration, iii) non-immunogenicity, iv) high thermal stability, v) low
539 cost and faster synthesis, and vi) easy modification (Chen *et al.*, 2016; Sun and Zu, 2015; Yoo *et al.*,
540 2019).

541 Aptamers belong to a class of short RNA or single-stranded DNA nucleic acids with a unique 3D
542 structure that is designed for the specific binding to their target. Concerning the synthesis, the
543 systematic evolution of ligands by exponential enrichment or SELEX is normally applied. This process
544 consists of five steps including: i) mixing the target with a random oligonucleotide library, ii)
545 separating target bound sequences, iii) amplifying the target-bound sequences to generate an
546 enriched library, iv) mixing the target with the new library for the next round of enrichment, and v)
547 sequencing the enriched aptamer sequences after a number of selection rounds (Sun *et al.*, 2014).

548 Besides promising advantages, there also remain some drawbacks of aptamers due to their innate
549 structure that might hinder *in vivo* application. The most relevant limitation is their degradation by
550 nucleases in biological fluids. However, the development in biochemistry can help solve this issue.
551 Many efficient solutions have been developed to improve impressively their nuclease stability such
552 as: i) the substitution of the 2'-OH RNA functional group with 2'-fluoro, 2'-amino or 2'-O-methoxy, ii)
553 the substitution of the phosphodiester backbone with boranophosphate or phosphorothioate, iii) the
554 substitution with phosphorodithioate and 2'-O-methyl in one nucleotide, iv) the locked nucleic acid
555 technology, and v) the generation of mirror RNA sequences (Sun and Zu, 2015).

556 In EGFR targeting with nanomedicines, anti-EGFR aptamers have been conjugated to different kinds
557 of NPs (Table 2). For instance, Ilkhani *et al* introduced an anti-EGFR aptamer with a high affinity ($K_d =$
558 2.4 nM) to citrate-coated gold NPs (AuNPs) for better detecting EGFRs in biological fluids (Ilkhani *et*
559 *al.*, 2015). Lv and colleagues constructed novel gene-drug co-delivery polymeric NPs functionalized
560 with anti-EGFR aptamers to improve the therapeutic index in drug-resistant lung cancer. In
561 comparison with the non-targeted NPs, a better drug delivery and efficient gene transfection
562 efficiency were achieved with the targeted NPs. Consequently, the EGFR positive non-small lung
563 cancer cells (PC-9 and H1975) treated with the targeted NPs encountered a remarkable proliferation
564 inhibition, a better induced apoptosis, a down regulation of target protein expression and an
565 enhanced drug cytotoxicity compared to cells treated with the unmodified NPs (Lv *et al.*, 2018).

566 In addition to their targeting properties, these “chemical antibodies” can also exhibit their
567 therapeutic potency once introduced onto NPs. Chen *et al* developed albumin-ciplastin NPs
568 conjugated with anti-EGFR aptamers for better efficacy and tolerability of cisplatin in the treatment
569 of EGFR positive cervical cancer. Both the free aptamers in solution and the conjugated aptamers on
570 NPs were able to bind specifically to the EGFR positive cervical cancer Hela cells. Moreover, a greater
571 tumor accumulation of cisplatin was obtained with the aptamer-functionalized NPs and resulted in a




572 significant reduction of the IC₅₀ of cisplatin (26 μM for the targeted NPs vs 55 μM for the free drug
573 or 56 μM for the non-targeted NPs). Better tumor accumulation also improved the tolerability of
574 cisplatin with less systemic toxicity and nephrotoxicity. Interestingly, the conjugated aptamers also
575 presented their therapeutic activity by blocking the EGFR activation and contributed to the antitumor
576 activity of the final NPs (Chen *et al.*, 2016).

577 Kang *et al* carried out an interesting study to compare the benefit of anti-EGFR aptamers and
578 cetuximab in EGFR-targeting activity with nanomedicines. In this study, two lipid NPs co-loading
579 paclitaxel and quantum dots were functionalized with cetuximab or anti-EGFR aptamers. Compared
580 to the non-targeted NPs, both the NPs functionalized with antibodies or aptamers clearly exhibited
581 higher localization in tumor tissues and enhanced the therapeutic efficacy with stronger tumor
582 inhibition by a factor of five. Although the binding affinity of the anti-EGFR aptamer is only a half of
583 that of cetuximab ($K_d = 0.62$ nM vs 0.38 nM, respectively) and the number of ligands per NP was
584 similar, the aptamer-NPs and the antibody-NPs demonstrated similar binding capacity to the target
585 cells. The authors proposed that due to the smaller size compared to that of cetuximab, the
586 conjugated aptamers might have a higher chance for multivalent interaction with EGFRs on target
587 cells than the conjugated cetuximab and could explain the similar binding activity despite its lower
588 binding ability. These results suggested that the interaction capacity between targeting ligands and
589 receptors is also important to their targeting ability and needs to be considered in the design step of
590 nanomedicines (Kang *et al.*, 2018).

591 A novel and efficient modality for EGFR positive cancers' treatment can be developed by the
592 functionalization of nanomedicines with anti-EGFR aptamers. Compared to other kinds of EGFR
593 ligands that are protein-based ones, anti-EGFR aptamers offer a unique advantage in terms of
594 thermal stability. This property may be very helpful for the future large-scale production and long-
595 term storage. Nevertheless, as aptamers can only target the receptors if they are in a correct
596 conformational structure, their conformation on the surface of NPs must be considered with
597 vigilance to select appropriate conjugation methods, and ensure their targeting properties.

598 **Table 2 EGFR-targeting ligand available for conjugation onto nanoparticles**

Targeting moiety	Structure	MW (KDa)	K _d (nM)	Advantages	Drawbacks	Ref.
EGF protein	A single polypeptide of 53 amino acids	6	1.0-2.0	Small size, natural ligand for EGFRs, low risk of immunogenicity, easy conjugation	High-cost and complicated production, susceptibility to hypersensitive reactions for the murine EGF	(Grapa <i>et al.</i> , 2019; Master and Sen Gupta, 2012; Negahdari <i>et al.</i> , 2016; Silva <i>et al.</i> , 2016)
Affibody	Scaffold protein of 58 amino acids	7	2.8	Low molecular weight and size, high stability, easy conjugation, low immunogenicity	Lower binding affinity compared to mAbs, lack of data on safety and short half-life time	(Lucky <i>et al.</i> , 2016; Y. Zhang <i>et al.</i> , 2018)
Repebody	Scaffold protein with a leucine-rich repeated module	30	9.18	Small size, better tissue penetration than mAbs	Lack of data on safety	(Pyo <i>et al.</i> , 2018)
Monoclonal antibody	<p>Antigen binding site Variable region Constant region V_H domain V_L domain C_{H1} + C_L domain C_{H2} C_{H3}</p>	150	Cetuximab : 0.39 Panitumumab : 0.05 Nimotuzumab : 4.53	Highest binding affinity, longest history of utilization, safety	Big size, limited number of conjugated ligands, high-cost production, immunogenicity, stability, rapid capture by liver and spleen	(Chu <i>et al.</i> , 2015; Kim and Grothey, 2008; Master and Sen Gupta, 2012; Ramakrishnan <i>et al.</i> , 2009)
Fab fragment	VH-VL via disulfide bonds 	50	5.6	Small size, easy production, low immunogenicity, high stability, longer circulation time than mAbs	Lower binding affinity than mAbs	(Alibakhshi <i>et al.</i> , 2017b; Zhai <i>et al.</i> , 2015)

ScFv fragment	VH-VL linked via a peptide linker 	25	3.36	Small size, high affinity, easy production, low immunogenicity, orientated conjugation	Lower binding affinity than mAbs	(Master and Sen Gupta, 2012; Yang <i>et al.</i> , 2009)
Nanobody	Camelid and shark VH 	15	5-20	Small size, high thermal and chemical resistance, high solubility, easy conjugation, low immunogenicity	Scale-up, difficulty in synthesis	(Master and Sen Gupta, 2012; Roovers <i>et al.</i> , 2011)
Bispecific antibody	Two scFv linked via the CH ₃ domain 	50	Comparable to corresponding scFv	Increased binding specificity, blockage of two different mediators, better conjugation and tumor penetration in NPs		(Cui <i>et al.</i> , 2019; Master and Sen Gupta, 2012)
GE11 peptide	Small peptide of 12 amino acids	1.5	22	Small size, low immunogenicity, easy synthesis, easy conjugation with good orientation	Lower affinity than mAbs	(Li <i>et al.</i> , 2005; Pi <i>et al.</i> , 2017)
Aptamer	Single stranded nucleic acid with a 3D specifically designed structure	8-25	2.4	Small size, better and faster tumor penetration, non-immunogenicity, high thermal stability, low cost and faster synthesis, possible surface modification	Nuclease degradation	(Chen <i>et al.</i> , 2016; Sun and Zu, 2015)

599

600

601

602 3. Methodologies involved in the conjugation of EGFR active targeting ligands onto NPs' surface

603 A wide variety of approaches have been developed to introduce targeting moieties onto nanocarriers
604 including both physical interactions and chemical conjugations. For EGFR targeting, the physical
605 method is normally based on physical adsorption or electrostatic interactions and chemical strategies
606 involving carbodiimide, maleimide and click chemistry. In the following section, the advantages and
607 drawbacks of each conjugation method will be *discussed*.

608 3.1. Non-covalent adsorption

609 The first and easiest conjugation method is to adsorb targeting ligands onto the surface of NPs via
610 non-covalent linkages. Non-covalent adsorption may be divided into physical adsorption and ionic
611 binding. Physical adsorption occurs via weak interactions such as hydrogen bonding, hydrophobic
612 and Van der Waals attractive forces, while ionic binding is based on the interactions between the
613 opposite charges of ligands and NPs (**Table 3**). Compared to other conjugation strategies, this
614 method provides several advantages including i) avoiding complex chemical conjugation that helps
615 preserve ligand biological activities, ii) easy and fast formulation, iii) fast release of the ligand in
616 tumor sites and possibility to deploy the ligand antitumor activities, iv) possibility to minimize the
617 cytotoxicity linked to highly charged NPs (Juan *et al.*, 2020; Li *et al.*, 2015a; Y. Zhang *et al.*, 2018).
618 Nevertheless, its weak stability in biological fluids due to weak interactions established between
619 ligands and NPs remains one of the biggest challenges for its *in vivo* applications. Among the
620 available targeting moieties for EGFR-targeting, this conjugation method can be applied to EGF
621 proteins (Li *et al.*, 2015a; Silva *et al.*, 2016; Zhang *et al.*, 2012); affibodies (Y. Zhang *et al.*, 2018);
622 repebodies (Kim *et al.*, 2018) and mAbs (Li *et al.*, 2015b; Lu *et al.*, 2018; Qian *et al.*, 2015). As charged
623 NPs are normally required in this strategy, dendrimers, gold nanoparticles (AuNPs) or cationic
624 liposomes are the most widely used. Consequently, the surface charges of the resulting NPs are
625 significantly changed in most cases compared to the non-targeted NPs. Thus, the change in the
626 surface charge of the ligand-conjugated NPs can serve as an indicator to confirm a successful
627 conjugation process.

628 In the ionic binding for positively charged NPs such as dendrimers, active targeting moieties need to
629 be negatively charged. As an example, Zhang *et al* succeeded in adsorbing negatively charged EGF
630 proteins onto highly positively charged dendrimers. The zeta potential of the finalized NPs declined
631 significantly from $+18.3 \pm 0.3$ mv to $+3.3 \pm 0.5$ mV, whereas the size remained unchanged around 350
632 nm (Zhang *et al.*, 2012). In another study, Kim *et al* introduced a polyanionic peptide to an anti-EGFR
633 repebody and then exploited the electrostatic interactions between the negative charges of this
634 peptide with the positive charges of dendrimers to formulate a final dendrimer complex for a
635 targeting gene delivery. The resulting dendrimer complex was also significantly neutralized in terms
636 of charge (Kim *et al.*, 2018). Always in order to introduce targeting ligands onto dendrimers, Li and
637 colleagues adsorbed h-R3 mAbs to PAMAM dendrimers and created final self-assembled h-R3-
638 PAPAM-DNA complexes. In this complexation, electrostatic associations were created between the
639 positively charged dendrimers and the negatively charged h-R3 and DNA (Qian *et al.*, 2015). In
640 addition to the targeting properties, conjugated ligands may play also the role of toxicity-reducing
641 agent for the highly charged dendrimers. In fact, the only possible way for non-targeted dendrimers
642 to enter the cell is through non-specific endocytosis that may damage the lipid bilayer structure of
643 the cell and cause cell death. On the contrary, neutralized dendrimers with conjugated ligands can
644 enter the cells through a non-specific pathway and also through the EGFR signal pathway endocytosis,
645 which is a normal physiological process. Therefore, the less charged NPs and the two internalization
646 pathways may cause less damage to the cell membrane than their counterparts may. This
647 phenomenon was confirmed in the studies of Zhang *et al* and Kim *et al* for EGF-conjugated and anti-

648 EGFR rebody-conjugated dendrimers, respectively. In these studies, an attenuated cytotoxicity
649 level related to an increase in the amount of anti-EGFR ligands on the NPs surface was recorded for
650 the targeted dendrimers (Kim *et al.*, 2018; Zhang *et al.*, 2012). However, in case dendrimers are used
651 for gene delivery, ligand adsorption to dendrimers might increase steric hindrance and electrostatic
652 repulsion against nucleic acids. To overcome these problems, the ratio of ligand/DNA or the orders of
653 the complexation need to be optimized. As an example, Li *et al* showed that the antibody/DNA ratio
654 needed to be inferior to five in order to complex completely DNA (Qian *et al.*, 2015). In another study,
655 Zhang and co-workers found that if EGF adsorption occurs after the formation of DNA-dendrimer
656 complexes, it did not affect the interaction of DNA-dendrimers (Zhang *et al.*, 2012). To conclude,
657 there are two possible solutions to tackle the hindrance of ligand adsorption to the complexation
658 between DNA and dendrimers including i) the use of an appropriate ratio of ligand/nucleic acid or ii)
659 the post-conjugation strategy of the charged ligand.

660 The positively charged anti-EGFR ligands can be also introduced onto negative metallic NPs such as
661 SPIONs, AuNPs or AgNPs via electrostatic interactions. Zhang *et al* used the electrostatic interactions
662 between positive charges of the histidine residues in anti-EGFR affibodies and negative charges of
663 COOH groups in quantum dots for the photoacoustic imaging of EGFR positive tumors. A remarkable
664 increase in the zeta potential from -37 mV to +0.31 mV was recorded after the affibody conjugation
665 that revealed the presence of affibody ligand (Y. Zhang *et al.*, 2018). For mAbs, Cetuximab possesses
666 an isoelectric point at $pH_i=8.48$. Therefore, Cet is positively charged in $pH < pH_i$ and negatively charged
667 in $pH > pH_i$ (Chu *et al.*, 2015). Therefore, a possible adsorption of Cet onto positively charged NPs can
668 be achieved in $pH < pH_i$.

669 Besides the ionic binding, physical adsorption can also be used to conjugate anti-EGFR fragments
670 onto NPs. However, the biggest issue of this method is that it is impossible to ensure the
671 functionality of the adsorbed antibodies on NPs surfaces. Moreover, due to the weak linkage
672 between the conjugated ligands and NPs, once these targeted NPs are in contact with the biological
673 fluids, a competition between ligands and the complex mixtures of serum or plasma proteins may
674 occur and the targeting ligands may be covered or replaced by these proteins (Tonigold *et al.*, 2018).
675 Despite its disadvantages, this strategy can be used in cases where no other methods are suitable.
676 Using this strategy, two studies of Lu *et al* and Qian *et al* conjugated Cetuximab onto Fe_3O_4 -AuNPs
677 and AuNPs, respectively. In this conjugation, the pH of the reaction medium was adjusted to the
678 isoelectric point of the antibody and a blocking treatment step with BSA (bovine serum albumin) was
679 performed to fix the conjugated ligands on the NPs surface. As a result, the targeted NPs in these
680 studies were able to target specifically the EGFR positive lung cancer (A549) and human glioma (U251)
681 cells, which confirmed the functionality of the adsorbed antibodies (Lu *et al.*, 2018; Qian *et al.*, 2015).

682 All the previous studies demonstrate the potential application of the non-covalent adsorption
683 strategy in the introduction of anti-EGFR ligands to NPs. However, its application remains limited due
684 to its weak stability. To overcome the challenge in the stability of non-covalent interactions, covalent
685 strategies have been developed.

686 **3.2. Carbodiimide chemistry**

687 Among available covalent strategies, carbodiimide chemistry is the most used, as synthetic schemes
688 are generally easy to carry out. This strategy refers to the reaction between carboxyl groups and
689 primary amine groups present in ligands and on the surface of NPs without the need of performing
690 any further chemical modification (**Table 3**). Before the reaction, the functional carboxyl groups must
691 be activated by the addition of cross-linking agents, where the free-length linker 1-ethyl-3-(3-
692 dimethylaminopropyl) carbodiimide (EDC) is the most used. However, only in an acidic medium (pH

693 4.5) that this reaction is the most efficient, and it must be performed in buffers devoid of extraneous
694 carboxyl groups and amine groups. In order to improve conjugation efficiency, N-
695 hydroxysuccinimide (NHS) or N-hydroxysulfosuccinimide (sulfo-NHS) are normally added (Juan *et al.*,
696 2020).

697 In terms of EGFR-targeting, carbodiimide chemistry can be used for most ligands such as EGF
698 proteins (Gill *et al.*, 2018; Tsai *et al.*, 2018), reprobodies (Lee *et al.*, 2017), mAbs (Huang *et al.*, 2015;
699 Maya *et al.*, 2013; Wang and Zhou, 2015), Fab fragments (Houdaihed *et al.*, 2020), bispecific
700 antibodies (Wu *et al.*, 2016), and aptamers (Chen *et al.*, 2016; Lv *et al.*, 2018; Xie *et al.*, 2019). Using
701 this strategy, Gill *et al* were able to conjugate EGF proteins in DTPA-EGF to their PLGA nanoparticles
702 via the reaction between primary amines on EGFs and carboxyl groups on the polymeric NPs. The
703 resulting nanoparticles allowed further complexation with a radioactive agent and the conjugation
704 yield was determined to be around 2 µg of EGF per mg of NPs (Gill *et al.*, 2018). In another study of
705 Lee *et al*, an anti-EGFR reproboddy was successfully conjugated to an oncolytic protein that could later
706 self-assemble into nanoparticles of around 48 nm via the reaction between NH₂ in reprobodies and
707 the COOH terminus of the protein. The resulting self-assembled nanoparticles showed a high
708 homogeneity and stability level in physical conditions (Lee *et al.*, 2017). In addition, Maya *et al* firstly
709 activated the carboxyl groups on O-carboxymethyl chitosan NPs and then conjugated them with the
710 amino groups of cetuximab. The Cet conjugation efficiency in this study was found to be 42±6 %
711 (Maya *et al.*, 2013). Using this strategy, Houdaihed and colleagues were also able to introduce an
712 anti-EGFR Fab onto COOH-PEG-PLGA NPs for a targeted delivery of paclitaxel into breast cancer cells.
713 The reaction occurred between the primary amine functions of Fab fragments and the carboxyls
714 groups of the polymeric NPs (Houdaihed *et al.*, 2020). For anti-EGFR aptamer conjugation, Lv *et al*
715 activated the COOH groups of anti-EGFR aptamers and subsequently coupled them with the NH₂-
716 terminated dendrimers to tackle drug resistance in non-small cell lung cancer (Lv *et al.*, 2018).

717 In the study of Yoon *et al*, instead of using physical adsorption to conjugate cetuximab onto
718 dendrimers as previously described, the authors applied the reaction between free primary amine
719 groups on the dendrimers and carboxyl groups on the Fc region of Cet that provided a better stability
720 level than non-covalent adsorption (Yoon *et al.*, 2016). The same observation was shown in the study
721 of Zhang *et al* to conjugate Cet onto dendrimers for EGFR targeting. The authors showed that the
722 multiple amino groups of dendrimers made them outstanding in the chemical conjugation of
723 antibodies and may enhance the yield as well as the stability of ligand conjugation in comparison
724 with electrostatic interactions (Zhang *et al.*, 2016).

725 Although this strategy is easy and does not require further chemical modification, the coupling
726 between functional groups and crosslinkers is not highly selective due to the abundance of primary
727 amines functions or carboxyl groups in ligands or NPs themselves or in biological fluids. Moreover,
728 the absence of control over the ligand orientation present on the NPs surface might hinder its
729 targeting properties (Juan *et al.*, 2020).

730 3.3. Maleimide chemistry

731 Recently, the maleimide chemistry has been widely exploited to functionalize NPs with active
732 targeting ligands. This strategy is based on the reaction between free sulfhydryl groups (-SH) on
733 ligands and maleimide groups on NPs to form a stable thioether linkage (**Table 3**). This strategy offers
734 several advantages compared to carbodiimide chemistry including i) much faster reactions and
735 efficiency at a neutral pH suitable for ligands or NPs with a low stability level in acidic media and ii)
736 better selectivity and ligand orientation on NPs due to the fact that functional groups are much less
737 abundant in biological fluids (Juan *et al.*, 2020).

738 As free sulfhydryl moieties are required in this method, two strategies can serve to generate free
739 sulfhydryl groups or the de-protonated form of thiol at physiological pH. The first way is via the
740 reduction of native disulfide bonds of the cysteine residues in ligands with reducing reagents. To this
741 end, dithiothreitol (DTT) and tris(carboxyethyl)phosphine (TCEP) are the most used reducing reagents
742 (Agarwal and Bertozzi, 2015). In addition, ligands can also be thiolated by modifying the primary
743 amine groups on lysine residues with sulfhydryl-addition reagents such as 2-iminothiolane (Traut's
744 reagent) and N-succinimidyl S-acetylthioacetate (SATA) (Yoo *et al.*, 2019; Yu *et al.*, 2012). On the
745 other side, to introduce maleimide groups on NPs, maleimide cross-linking reagents such as
746 NHS/maleimide heterobifunctional linkers are normally used. A wide variety of linkers can be applied
747 including PEGylated analogues (NHS-PEG-maleimide), succinimidyl 4-(N-
748 maleimidomethyl)cyclohexane-1-carboxylate (SMCC) and sulfosuccinimidyl 4-(N-
749 maleimidomethyl)cyclohexane-1-carboxylate (sulfo-SMCC). Among these linkers, PEGylated
750 analogues are preferred in nanomedicines due to the resulting improving stealthiness effect (M.
751 Cardoso *et al.*, 2012).

752 Maleimide chemistry can be used for nanoconjugation with all kinds of EGFR-targeting ligands
753 mentioned in this review. As an example, Faucon *et al* firstly introduced maleimide units onto the
754 surface of NPs using N-(maleimidoethyl) amine via carbodiimide chemistry. Subsequently, free
755 sulfhydryls were generated using DTT from the six cysteine residues in the EGF structure and reacted
756 with maleimide-functionalized NPs. The resulting NPs possessed around 4.7 EGF ligands per NP
757 (Faucon *et al.*, 2017). In another effort to conjugate anti-EGFR affibodies onto upconversion NPs for
758 photodynamic therapy in solid oral cancers, Lucky and colleagues transformed the non-activated
759 thiols in cysteine-residues of affibodies into activated thiols with the reducing agent DTT and
760 subsequently conjugated them to the bifunctional maleimide-PEG-COOH linker via thioether bonds.
761 Afterwards, the nanoparticles were coated by the silane groups to provide primary amine groups,
762 which allowed subsequent conjugation with carboxyl groups in affibody-PEG (Lucky *et al.*, 2016).
763 Kang and co-workers managed to conjugate cetuximab and an anti-EGFR aptamer onto lipid micellar
764 NPs for co-loading quantum dots and paclitaxel. In this study, sulfhydryl groups were introduced into
765 Cet or aptamers via the reaction with the Traut's reagent and then the thiolated ligands reacted with
766 maleimide groups on lipid micelles. Interestingly, the number of conjugated ligands was the same for
767 cetuximab and the anti-EGFR aptamer (Kang *et al.*, 2018). Our group also succeeded in developing
768 theranostic EGFR-targeting NPs with a humanized anti-EGFR scFv. In our study, a cysteine-tag was
769 introduced into the C-terminus of our anti-EGFR scFv and the NPs were previously coated by an NHS-
770 PEG-Mal polymer layer. After the reduction with TCEP to generate free sulfhydryls, the activated
771 scFvs were conjugated onto our NPs via maleimide chemistry. The number of anti-EGFR scFv was
772 determined to be around 13 scFvs per SPION (Vinh Nguyen *et al.*, 2020).

773 In addition to protein ligands, maleimide chemistry was also applied for GE11 peptide and anti-EGFR
774 aptamers. In fact, GE11 is usually grafted with four glycine residues as the spacer and a terminal
775 cysteine (GGGGC) that allows the application of maleimide chemistry. As an example, Chariou *et al*
776 firstly grafted a bifunctional PEG linker onto their virus-based nanoparticles (VNPs) and subsequently
777 linked them with the cysteine-terminated GE11 for the detection and imaging of various kinds of
778 EGFR-overexpressed cancers including skin epidermoid carcinoma (A431), colorectal cancer (HT-29)
779 and triple-negative breast cancer (MDA-MB-231) (Chariou *et al.*, 2015). In another study, Kim and co-
780 workers used maleimide chemistry to introduce anti-EGFR aptamers onto a liposomal system for co-
781 delivering quantum dots and nucleic acids. Aptamers were thiolated with the DTT reagent and then
782 reacted with the maleimide groups present on liposomes. The resulting liposomes were shown to be
783 efficient as nanocarriers for tumor-directed gene delivery and bio-imaging (Kim *et al.*, 2017).

784 Furthermore, maleimide chemistry also appears as a good alternative in case carbodiimide chemistry
785 is not appropriate due to the accessibility issue of functional groups on NPs/ligands or aggregation
786 problems because of acidic pH. As an example, Lee and co-workers developed Cet-conjugated
787 quantum dots for cancer imaging using the maleimide strategy instead of the carbodiimide one. The
788 carboxylated polymer-coated quantum dots were modified into amine via reactions with diamino-
789 PEG and subsequently thiolated by a reducing reagent DTT. On the other side, the cetuximab
790 antibody was activated and conjugated to one side of sulfo-SMCC. Finally, free thiol groups on the
791 activated nanoparticles were connected to maleimide groups on the other end of sulfo-SMCC. As a
792 result, approximately 6 cetuximabs per NP were introduced onto the finalized NPs (Lee *et al.*, 2010).

793 Despite its robust covalent conjugation with a greater stability level than the non-covalent
794 approaches and better selectivity than the carbodiimide strategy, maleimide chemistry also suffers
795 from several issues. Especially, the thiolation step may change the chemical structure of the ligand
796 and hinder its binding affinity. Furthermore, the non-selectivity of maleimide to cysteine-rich
797 reaction media has also been reported. This lack of selectivity is due to exchange reactions with thiol-
798 containing proteins in serums. As a result, non-homogenous conjugates and poorly defined yielding
799 off-target cytotoxicity may occur (Juan *et al.*, 2020).

800 **3.4. Click chemistry**

801 To tackle the problem of non-selectivity in the ligand conjugation, site-specific conjugation strategies
802 such as click chemistry is one of the most suitable approaches (Table 3). Click chemistry refers to the
803 formation of a stable triazole linkage by the reaction between alkyne and azide groups. To do so, a
804 linker is normally used to connect ligands and NPs. In most cases, the functionalization of NPs or
805 ligands with azide or alkyne moieties goes through carbodiimide or maleimide conjugation.
806 Therefore, NHS esters or maleimide groups needs to be present on one side of the linker, while azide
807 or alkyne groups must be located on the other side. Compared to the previous methods, this reaction
808 can occur under mild conditions (in aqueous solvents at room temperature), does not require
809 sophisticated purification and provide irreversible chemical bonds with the absence of cytotoxic
810 byproducts (Juan *et al.*, 2020). Moreover, thanks to the low presence of these functional groups in
811 biological systems or biomolecules, this strategy can be exempt from undesirable reactions with
812 other functional groups and provides a specific conjugation at the desired location on the
813 biomolecules. Therefore, a highly oriented ligand conjugation can be achieved and click chemistry is
814 highly recommended for the functionalization of NPs with targeting moieties. However, the original
815 kind of this strategy requires the presence of a Cu(I) catalyst, which is susceptible to toxicity. Recently,
816 Weisseleder *et al* have developed a novel cooper-free click chemistry procedure to overcome the
817 toxicity linked to Cu(I)-catalyzed reaction by exploiting the reaction between azide and alkyne groups
818 in trans-cyclooctene (TCO).

819 This conjugation method is attracting an increasing interest and more and more applied in
820 nanoconjugation approaches involving EGFR-targeting NPs. As an example, Kotagiri and co-workers
821 constructed a cooper-free chemical process to conjugate cetuximab onto their quantum dots for a
822 rapid analysis of biological samples. On one side, amine-coated quantum dots were activated with an
823 NHS-PEG-Azide cross-linker. On the other side, cetuximab was functionalized with NHS-PEG-
824 dibenzocyclooctyne (NHS-PEG-DBCO). These intermediate products then engaged in a click reaction
825 to obtain the finalized antibody-decorated quantum dots (Ab-QD) with a high yield (around 88 %).
826 Interestingly, the authors also prepared different Ab-QD NPs as comparative NPs, using traditional
827 strategies such as maleimide chemistry with the SMCC linker or the biotin-streptavidin strategy. The
828 recorded number of conjugated antibodies from click chemistry was two times and five times higher
829 than those of the maleimide and the biotin-streptavidin strategies, respectively (8.4 vs 3.9 and 1.6

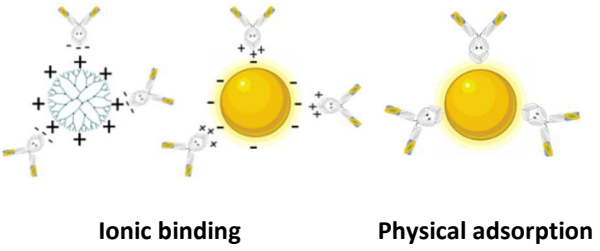
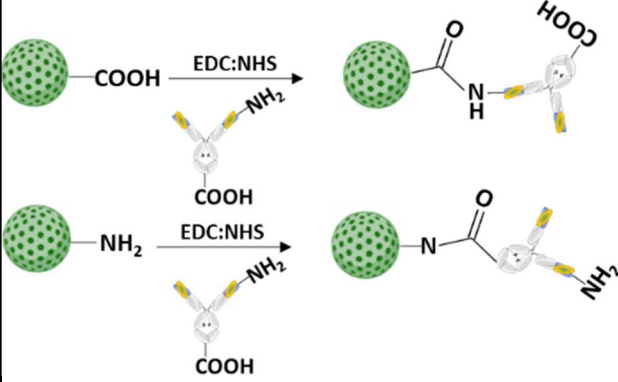
830 antibody per QD). Moreover, Cet-QD NPs with click chemistry showed a better binding ability to
831 EGFR positive human pancreatic and breast cancer cells (BxPc-3 and MDA-MB-231, respectively) than
832 Cet-NPs prepared with other strategies. These results suggested that click chemistry was more
833 selective with a higher yield and improved the orientation of conjugated ligands on the NPs surface
834 resulting in a better binding affinity towards EGFRs on the cell surface (Kotagiri *et al.*, 2014).

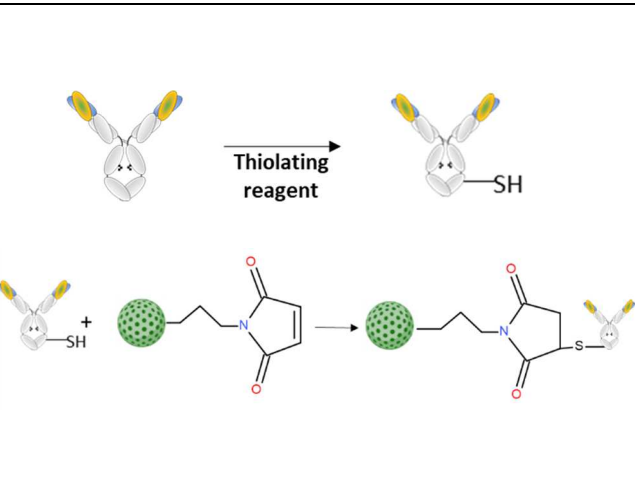
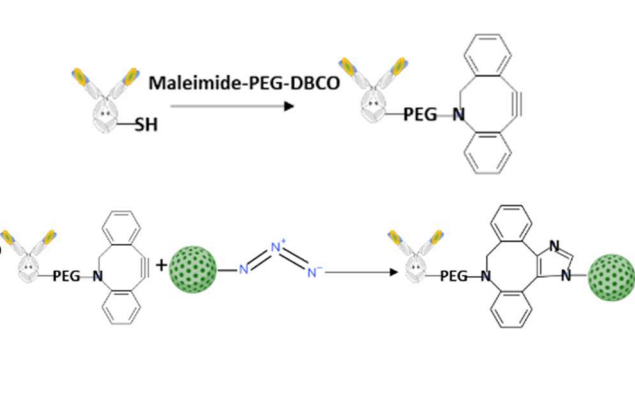
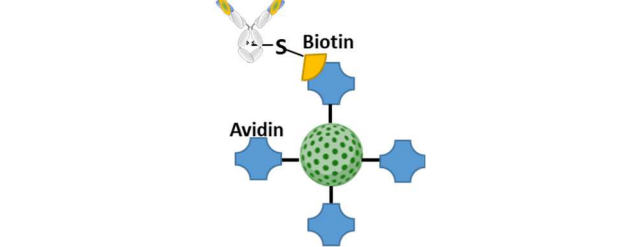
835 Despite its high conjugation yield and high selectivity, few studies have applied click chemistry for
836 nanoconjugation with EGFR-targeting ligands so far. This chemical strategy is relatively new and
837 more complicated than traditional methods. Furthermore, while the reaction between alkyne and
838 azide groups is highly specific, the introduction methods of these functional groups onto targeting
839 ligands or NPs normally involves classical conjugation chemistries such as carbodimide or maleimide
840 ones. As these conventional chemistries are not entirely specific, a careful consideration on this
841 aspect is necessary, especially in the case of targeting ligands that require highly conformational
842 structure for targeting properties such as aptamers. In all cases, click chemistry has proved its great
843 potential for the conjugation of targeting moieties to nanoparticles.

844 **3.5. Non-covalent binding by adapter molecules**

845 The study of Kotagiri and co-workers also suggested another selective conjugation strategy for EGFR
846 targeting NPs that is based on another non-covalent approach using adapter biomolecules. This
847 strategy can help avoid randomly oriented antibodies and enhanced the stability of linkage. The most
848 relevant used method in this strategy exploits the strong binding affinity between biotin and a biotin-
849 binding protein such as avidin or its analogues (Juan *et al.*, 2020). As biotin and avidin need to be
850 present on ligands and NPs, other chemical strategies are normally applied to conjugate these
851 moieties. Despite its potency, this conjugation strategy has not been applied so far to introduce anti-
852 EGFR ligands onto NPs. Nevertheless, it promising application was demonstrated with similar
853 receptors such as HER2. Warlick and colleagues managed to prepare targeted NPs for HER2 active
854 targeting using biotin/neutravidin. In this study, an anti-HER2 antibody (trastuzumab) was
855 biotinylated using carbodiimide chemistry and maleimide chemistry was used to functionalize
856 albumin NPs with neutravidin. As a result, specific targeting to HER2-overexpressing cells was
857 obtained (Wartlick *et al.*, 2004). This study demonstrated the perspective of applying the biotin-
858 avidin strategy to functionalize NPs with anti-EGFR fragments.

859 **Table 3 Available conjugation strategies for the functionalization of nanoparticles with anti-EGFR ligands**

Conjugation strategy	Mechanism	Appropriate EGFR-targeting ligands	Appropriate NPs	Advantages	Drawbacks	Ref.
Non-covalent adsorption	 <p style="text-align: center;">Ionic binding Physical adsorption</p>	EGF proteins, affibodies, reprobodies, mAbs	Charged NPs such as dendrimers, AuNPs, AgNPs	Fast and easy formulation; avoidance of complex chemical conjugation; release of ligands in the tumor with antitumor activity; reduced toxicity due to high charges of NPs	Weak interactions and stability	(Krishnamurthy and Jimeno, 2018; Pi <i>et al.</i> , 2017; Wu <i>et al.</i> , 2016; Yoo <i>et al.</i> , 2019)
Carbodiimide chemistry		EGF proteins, reprobodies, mAbs, Fabs, bispecific antibodies, peptides, aptamers, etc.	Micelles made of polymers, amphiphilic molecules, lipids; chitosan NPs; liposomes; inorganic NPs, etc.	High stability; higher conjugation efficiency than the physical method; no chemical modification on the ligands	Low selectivity; absence of control over ligand orientation; reactions in acidic and water-free media	(Holliger and Hudson, 2005; Lv <i>et al.</i> , 2018; Roovers <i>et al.</i> , 2011; Talekar <i>et al.</i> , 2016; Tsai <i>et al.</i> , 2018; Yook <i>et al.</i> , 2015)
Maleimide		EGF proteins;	Micelles	Faster and more	Thiolation	(Chariou <i>et</i>

chemistry		<p>affibodies; repebodies; mAbs; Fabs; scFvs; nanobodies; bispecific antibodies; GE11 peptide; aptamers</p>	<p>made of polymers, amphiphilic molecules, lipids; chitosan NPs; liposomes; inorganic NPs, etc.</p>	<p>selective reactions; neutral pH media that avoid NPs aggregation</p>	<p>may hinder biological activities of ligands; non-selectivity in thiol-containing media</p>	<p>al., 2015; Faucon et al., 2017; Juan et al., 2020; Kang et al., 2018; Kim et al., 2017; Lucky et al., 2016; Sandoval et al., 2012)</p>
Click chemistry		<p>EGF proteins; affibodies; repebodies; mAbs; Fabs; scFvs; nanobodies; bispecific antibodies; GE11 peptide; aptamers</p>	<p>Micelles made of polymers, amphiphilic molecules, lipids; chitosan NPs; liposomes; inorganic NPs, etc.</p>	<p>Site-specific conjugation; higher yield; control of ligand orientation; mild conditions, unsophisticated purification</p>	<p>Relatively new and more complicated than other methods; possible toxicity with Cu(I) catalysts</p>	<p>(Juan et al., 2020; Kotagiri et al., 2014; Yu et al., 2012)</p>
Biotin-avidin		<p>Not applied yet for EGFR</p>	<p>Most of kinds of NPs</p>	<p>Good orientation of conjugated ligands</p>	<p>Non-covalent strategy and more complicated than other methods</p>	<p>(Juan et al., 2020)</p>

860 4. Main analytical methods used for detecting the presence of conjugated ligands on the surface 861 of NPs

862 Following ligand conjugation, analytical methods are necessary to confirm whether the ligand is
863 successfully introduced onto NPs or not. Currently, most studies are relying on the changes in NPs'
864 physico-chemical properties (e.g., their size and charge) as indicators of successful conjugation.
865 Nevertheless, to the best of our knowledge, such indicators are not sufficient, and in some cases,
866 might even be misleading. The following part of this review is designed to provide information on the
867 available analytical methods for the detection of conjugated anti-EGFR ligands on NPs.

868 4.1. Size and charge of the nanoparticles

869 The introduction of a ligand to NPs might lead to an increase in their size and a change in their
870 surface charge, compared to those of the bare NPs. Such changes in physico-chemical properties may
871 be indicators of successful conjugation.

872 In terms of size, the hydrodynamic diameter (D_H) is normally used and can be determined using the
873 dynamic light scattering (DLS) method. Other techniques for size determination such as TEM images,
874 in most cases, are not appropriate for detecting the presence of conjugated ligands. In EGFR-
875 targeting, an increase in D_H is particularly noticeable when large-size ligands such as whole antibodies
876 (e.g., cetuximab, whose size is around 10-15 nm) are conjugated. As an example, the polymeric NPs
877 in the study of Wang et Zhou increased in size from 105 nm to 122 nm after antibody-conjugation
878 (Wang and Zhou, 2015). An increase in size (from 175 nm to 185.7 nm) was also used to reveal the
879 presence of Cet on the liposome surface in the study of Liu and colleagues (Liu *et al.*, 2019). In the
880 study of Maya *et al.*, after Cet conjugation, the size of their chitosan NPs dramatically increased from
881 130 ± 25 nm to 180 ± 35 nm (Maya *et al.*, 2013). In our opinion, this large increase in size (around 50
882 nm) may come not only from the introduction of Cet onto the NPs, but also from other factors such
883 as nanoparticles' aggregation. Apart from whole antibodies, other anti-EGFR targeting ligands are, in
884 most cases, relatively small, making the DLS method not sensitive enough to distinguish the
885 difference in size before and after ligand conjugation. For example, our team managed to conjugate
886 an anti-EGFR scFv ligand onto SPIONs but there was no significant difference in the size of NPs after
887 the conjugation (Vinh Nguyen *et al.*, 2020). Zhai *et al.* observed a similar phenomenon for the
888 conjugation of an anti-EGFR Fab that was the second biggest kind of anti-EGFR fragments onto their
889 lipid NPs. The authors found that this conjugation barely changed the size of the NPs, which
890 remained around 230 nm (Zhai *et al.*, 2015). On the contrary, using the similar kind of ligand (anti-
891 EGFR Fabs) for their lipid NPs, Zhou *et al.* detected an increase in size from 96.3 nm to 111.7 nm after
892 Fab conjugation (Zhou *et al.*, 2007). These studies demonstrate that using only an increase in the size
893 of NPs may not be sufficient to confirm the presence of conjugated ligands.

894 Similarly to the size of NPs, the surface charge may also be modified after ligand conjugation. To
895 evaluate surface charges, measuring the zeta potential is the most widely used technique, as a clear
896 change in this parameter is usually recorded in non-covalent conjugation methods. Lu *et al.* carried
897 out a standard example by adsorbing Cetuximab on NPs. The zeta potential of their Fe_3O_4 -Au NPs
898 was totally reversed from -23.2 ± 1.8 mV for the bare NPs to $+11.1 \pm 1.8$ mV for the Cet-conjugated
899 NPs (Lu *et al.*, 2018). Besides, a change in the zeta potential was also observed for other kinds of
900 EGFR-targeting ligands using electrostatic forces. For instance, in the study of Yin and co-workers, the
901 authors constructed self-assembled complexes of the EGF protein, DNA and dendrimers. While the
902 size was almost unchanged, the zeta potential declined significantly from $+16.2 \pm 0.2$ mV to $+2.4 \pm$
903 0.8 mV, in line with an increasing ratio of EGF/DNA (Zhang *et al.*, 2012). Zhang and colleagues
904 decorated their negatively-charged quantum dots with positive anti-EGFR affibodies. As a result, the

905 zeta potential dramatically increased from -37 mV to +0.31 mV, which demonstrated successful
906 conjugation (Y. Zhang *et al.*, 2018). In the case of other conjugation strategies, the zeta potential may
907 be either unvaried or changed. For example, Sandoval *et al* conjugated the EGF protein onto their
908 liposomal NPs using maleimide-thiol chemistry. However, no difference in the zeta potential before
909 and after EGF conjugation was observed (Sandoval *et al.*, 2012). In our previous publication, the zeta
910 potential of NPs also remained at the same value, despite the successful introduction of an anti-EGFR
911 scFv ligand onto NPs using maleimide chemistry (Vinh Nguyen *et al.*, 2020).

912 In conclusion, an increase in the size of NPs or changes in their zeta potential after ligand conjugation
913 might prove the presence of a ligand on the NPs' surface, especially in the case of antibody
914 conjugation and conjugation methods using electrostatic interactions, respectively. Although many
915 studies in the field of nanomedicines are currently using these methods, such physico-chemical
916 property changes are insufficient, and other accurate techniques are required.

917 **4.2. Spectroscopic analysis**

918 Using spectroscopic analyses such as Fourier transform infrared (FT-IR) spectroscopy to analyze NPs
919 before and after ligand conjugation may help confirm successful coupling.

920 FT-IR analyses rely on the detection of special functional groups that are not present on NPs before
921 the conjugation and are only introduced onto NPs because of the presence of targeting ligands. The
922 apparition of these functional groups may be due to i) available groups present on ligands
923 themselves such as amine or carboxyl groups, ii) a new linkage established due to chemical
924 conjugation such as amide or thioether linkages, iii) functional groups on other molecules that are
925 linked beforehand to the ligand such as PEGylated ligands. FT-IR analyses have been deemed suitable
926 for detecting successful conjugation onto inorganic NPs using biological ligands. As an example,
927 Zhang *et al* confirmed the successful functionalization of their quantum dots with anti-EGFR
928 antibodies by means of FT-IR analyses combined with the detection of physico-chemical property
929 changes. In fact, the amine and the carboxyl groups from the conjugated antibodies were detected by
930 the peaks at 1645 cm^{-1} and 1538 cm^{-1} for the N-H stretching and N-H bending of the amine group,
931 respectively; and at 1715 cm^{-1} and 1345 cm^{-1} for the C=O and C-O stretching of the carboxyl group,
932 respectively (Y. Zhang *et al.*, 2018). In another study, Lucky and co-workers used FT-IR analyses to
933 confirm the successful grafting of PEGylated antibody conjugates on the surface of their TiO₂-
934 upconversion NPs. On one hand, the characteristic peaks of PEG at 2885 and $1470\text{-}1350\text{ cm}^{-1}$,
935 corresponding to C-H stretching and C-H bending, appeared after the grafting. On the other hand,
936 the presence of an amide linkage created after the conjugation was detected at 3500 and 1690 cm^{-1} ,
937 corresponding to N-H stretching and C=O stretching (Lucky *et al.*, 2016). Chen and colleagues
938 analyzed the FT-IR spectra of the NPs before and after the conjugation to confirm the presence of
939 anti-EGFR aptamers on their albumin NPs. The characteristic peaks of an amide linkage confirmed
940 the crosslink between aptamers and albumin NPs after the conjugation (Chen *et al.*, 2016).

941 However, this method is not always feasible due to possible weak signals of linkages created from
942 the conjugation. Furthermore, a suitable purification method is necessary to eliminate all non-
943 reacted ligands.

944 **4.3. Thermogravimetric analysis**

945 Thermogravimetric analyses (TGA) also appear among the analytical methods that might be used to
946 confirm the presence of EGFR-targeting ligands on the NPs' surface. As this method is based on the
947 weight loss of samples according to an increased temperature, it might be used to evaluate the
948 characteristic weight loss profile of the NPs before and after ligand conjugation due to the organic

949 content. Similarly to spectroscopic analyses, TGA are more suitable to confirm the presence of
950 organic ligands conjugated to inorganic NPs rather than in organic NPs.

951 Marega and co-workers carried out a good example for the application of TGA in EGFR-targeting NPs.
952 The authors managed to conjugate cetuximab onto their nanozeolites and used TGA to confirm this
953 coupling. TGA results showed that in the non-targeted nanozeolites (Zeo-NH₂), the amount of the
954 organic content and the oligoethylene-derived pyrolysis product was low, but increased significantly
955 in the targeted-NPs (Cet-Zeo-NH₂) due to the presence of cetuximab. Moreover, the characteristic
956 weight loss profile (minimum at 320 °C) obtained from the Cet-conjugated NPs confirmed the
957 presence of the antibody on the surface of NPs. Interestingly, this strategy also allowed the authors
958 to estimate the quantity of the grafted cetuximab in NPs (1.7-2.0 nmol of Cet per mg of NPs) (Marega
959 *et al.*, 2016).

960 **4.4. Structural and elemental analysis**

961 Recently, precise techniques such as structural or elemental analyses with ¹H-NMR or X-ray
962 photoelectron spectroscopy (XPS), respectively are increasingly used to verify qualitatively the
963 presence of biological ligands on NPs.

964 ¹H-NMR can be used to confirm the chemical structure of monomers used for further
965 nanoformulation, especially in the case of targeted micelles and liposomes. As an example, Nan *et al*
966 used this strategy to confirm the successful conjugation of the EGF protein onto PEGylated
967 phospholipid (PEG-DSPE) molecules by means of the maleimide chemistry, after which their EGFR-
968 targeting liposomes were constructed. The results obtained from ¹H-NMR spectra presented
969 chemical structure shifts, in comparison with the initial monomer (before the conjugation).
970 Furthermore, the structure of the ligand-functionalized monomer was confirmed with ¹H-NMR
971 spectra (Nan, 2019).

972 The introduction of organic ligands onto inorganic NPs normally results in an increase in organic
973 components in the finalized NPs and can be detected with XPS elemental analyses. In fact, once a
974 ligand is successfully coupled to non-organic NPs, C1s and O1s peak areas in XPS analyses will
975 increase significantly. Moreover, the presence of new elements such as N or S atoms due to ligand
976 coupling may also reveal the presence of active targeting moieties. In the study of Yamamoto and co-
977 workers on the conjugation of cetuximab onto gold NPs, the authors found that when the AuNPs
978 surface was functionalized with the EGF protein, the C1s and O1s peak areas increased significantly
979 (12.1 to 22.2 for C_{1s} and 6.14 to 13.0 for O_{1s}) (Yamamoto *et al.*, 2019). Marega and colleagues used
980 XPS spectra and TGA to confirm the coupling of cetuximab on their nanozeolites (Zeo-NH₂ NPs).
981 Before the conjugation, the XPS spectrum of Zeo-NH₂ NPs showed their expected elemental
982 composition including O, Si, Al, C for the ethylene glycol and N atoms of the terminal amino groups
983 (fewer than 1 % of N atoms). After the conjugation, the XPS spectrum clearly displayed the presence
984 of C-centered peaks that fingerprinted both the remained ethylene glycol on Zeo-NH₂ NPs and the
985 polypeptidic molecular fragments from the conjugated antibodies. Moreover, an enhanced content
986 of N atoms (around 11 %) coming from the conjugated cetuximab was recorded, denoting the
987 occurrence of bioconjugation. In addition, this analytical method may also help compare the
988 conjugation efficiency of two different conjugation strategies. In the same study *Marega et al.*, by
989 comparing the “organic to inorganic” proportion of the targeted NPs prepared with covalent
990 chemistry and that obtained from non-covalent adsorption of the antibody, the authors were able to
991 compare the yield of the non-covalent and the covalent methods. In fact, the sum of the percentage
992 of C1s and N1s divided by the sum of the percentage of Si2p and Al2p for each kind of NPs was
993 calculated. This ratio remained at the value of 4.0 for the antibody-conjugated NPs with non-covalent

994 or covalent strategies, suggesting that the conjugation yield of these strategies was similar in this
995 study (Marega *et al.*, 2016).

996 Despite their high precision, these techniques in most cases are unfeasible due to the small quantity
997 of conjugated targeting moieties present on NPs. Furthermore, a good purification method is
998 essential to preclude any interference of non-conjugated ligands. Nevertheless, these methods can
999 provide a firm conclusion on the presence of targeting ligands on NPs and worthy of consideration.

1000 **4.5. Fluorescence spectroscopy and imaging**

1001 A more selective and illustrating method for the detection of conjugated ligands is based on
1002 fluorescence spectroscopy. There are two available strategies for such detection. The first solution is
1003 to use a secondary antibody that is previously fluorescence-labeled and that can bind to the
1004 conjugated ligand. In this strategy, the targeted NPs are firstly incubated with the fluorescence-
1005 labeled antibody to create an antibody-ligand-NPs complex. This complex can be further detected
1006 thanks to fluorescence signals on the antibody. Besides, targeting ligands can also be previously
1007 fluorescence-labeled with a fluorescent dye that, once grafted onto NPs, can be detected by means
1008 of fluorescence spectroscopy.

1009 Lu *et al.* conjugated cetuximab onto Fe₃O₄@Au NPs using physical adsorption and the presence of
1010 cetuximab was confirmed with the use of fluorescence spectroscopy. The targeted NPs were first
1011 incubated with the FITC-conjugated anti-Human IgG to form the FITC-anti IgG-Cet-NPs complex. Then,
1012 the fluorescence from FITC on this complex was detected by a confocal laser-scanning microscope. A
1013 green fluorescence signal was observed for the targeted NPs, whereas no fluorescence was detected
1014 in the case of the non-targeted NPs (Lu *et al.*, 2018).

1015 In another effort to confirm the presence of coupled anti-EGFR aptamers on their dendrimers, Lv and
1016 co-workers introduced a fluorescence dye (FAM dye) onto the 3' terminal of their anti-EGFR
1017 aptamers with excitation and emission wavelengths at 491 nm and 519 nm, respectively. After the
1018 aptamer-conjugation, fluorescence signals of the FAM dye were revealed for all aptamer-modified
1019 NPs, but not with the bare NPs. This result indicated that aptamers were successfully introduced
1020 onto the NPs. Moreover, conjugation efficiency could also be estimated using the calibration curves
1021 of FAM-modified aptamer solutions. As a result, conjugation efficiency was found to be around 20 %
1022 in this study (Lv *et al.*, 2018). In another study of Xie and colleagues, the authors conjugated cyanine-
1023 modified aptamers onto their mesoporous silica NPs. By following the cyanine fluorescence signal,
1024 the authors were able to determine both qualitatively and quantitatively the grafted aptamers on
1025 NPs. In this study, each NP was shown to have around 344 aptamers on its surface (Xie *et al.*, 2019).
1026 However, as the non-conjugated ligands can interfere or even misinform the success of the
1027 conjugation, an appropriate strategy of purification plays an important role.

1028 Although its promising application has been proved, the introduction of a fluorescent dye onto EGFR
1029 targeting ligands may significantly change their structure, and results in a decrease in their targeting
1030 ability towards EGFRs. As a result, while applying this strategy, a complementary step of verifying the
1031 binding affinity of ligands before and after the introduction of fluorescent dye is necessary.

1032 **4.6. SDS gel electrophoresis**

1033 Among the available methods for the detection of ligands derived from proteins, one of the most
1034 efficient methods is sodium dodecyl sulfate-polyacrylamide gel electrophoresis (SDS-PAGE). The
1035 principle of this technique is based on the non-migration or retarded migration of nanoparticles in
1036 gels that allows the separation of unattached ligands from conjugated ones. In this technique, gel

1037 electrophoresis is performed with the targeted NPs, the non-targeted NPs as negative controls and
1038 solutions containing free ligands as positive controls. After the migration, the protein-staining
1039 reagent is added to reveal the presence of the protein. If the conjugation is successful, no protein
1040 band is observed for the targeted NPs at the location found using the free ligand solution, as it has
1041 already been co-localized with NPs. Using this strategy, Gill *et al* confirmed the conjugation of the
1042 EGF protein onto their polymeric NPs. In this study, after the revelation with the protein-staining
1043 reagent, the band corresponding to the free EGF protein (at MW = 6.4 kDa) appeared at the bottom
1044 of the gel and was used as the positive control. For the targeted NPs, that band was absent, but a
1045 strong protein band at the top of the gel co-localizing with the NPs confirmed the successful
1046 conjugation (Gill *et al.*, 2018).

1047 In addition to the application as a qualitative method, SDS-PAGE can also be used to estimate the
1048 quantity of the grafted ligands. To this end, serial dilution of ligand solutions is conducted to
1049 construct a calibration curve for the determination of conjugated ligands. Using this method, Kao and
1050 colleagues showed that around 124 cetuximab molecules per NP were coupled onto their AuNPs for
1051 an EGFR-targeting theranostic strategy (Kao *et al.*, 2013). In another study of Zhai and co-workers,
1052 the authors used SDS-PAGE to confirm the presence of conjugated anti-EGFR Fabs on their NPs and
1053 then used integrated images analyses to estimate the efficiency of this ligand conjugation (Zhai *et al.*,
1054 2015). However, image analyses do not seem to provide precise results. In our point of view, this
1055 method should only be used as a qualitative method or a control on the conjugation yield.

1056 **4.7. Protein dosage**

1057 For active targeting ligands with a protein origin, protein assays such as BCA and Bradford assays are
1058 widely used to estimate the quantity of the grafted ligands on the NPs surface.

1059 The BCA (bicinchonic) protein assay is a widely used method for the colorimetric detection and
1060 quantification of total protein in a solution. This Copper-based protein assay was introduced for the
1061 first time in 1985, involving two steps including protein-copper chelation and reduced copper
1062 detection. The resulting complex in BCA is water-soluble and exhibits a strong linear absorbance at
1063 562 nm with increasing protein concentrations. BCA is sensitive and has a broad dynamic range with
1064 capability of measuring protein concentrations from 0.5 µg/mL to 1.5 mg/mL. In addition, BCA is
1065 stable under alkaline conditions, and can be included in copper solutions to allow a one-step
1066 procedure. However, substances that reduce proteins or chelate copper also produce colors in the
1067 BCA assay, thus interfering with the accuracy of protein quantitation. This interference is also
1068 observed for certain single amino acids (such as cysteine, tyrosine and tryptophan). Therefore, the
1069 presence of these substances needs to be avoided in BCA assays (Walker, 2009).

1070 Another protein assay method that can be used for ligand quantification is the Bradford protein
1071 assay. The Bradford method is a dye-based assay that exploits the binding ability of the Coomassie
1072 blue to proteins. In acidic environments, proteins bind to the Coomassie dye and a spectral shift from
1073 the red form of the dye (maximal absorbance at 465 nm) to its blue form (maximal absorbance at
1074 610 nm) can be observed. Although the difference between the two forms of the dye is the greatest
1075 at 595 nm, this wavelength can be adjusted to be suitable for each solution. In terms of measuring
1076 capability, the Bradford assay is linear in a range of protein concentrations up to 2.0 mg/mL.
1077 Compared to other methods such as BCA, Bradford's is considered the fastest and the easiest
1078 method. Moreover, it is also compatible with most salts, solvents, buffers, thiols, reducing reagents
1079 and metal chelating agents.

1080 In the case of NPs functionalization using targeting ligands, both the BCA and the Bradford methods
1081 can be used, but each method has its own advantages and drawbacks. Therefore, the choice of a

1082 quantification method should be meticulously considered and can be based on i) the compositions of
1083 samples, ii) the stability and solubility of NPs in each method conditions, and iii) the required
1084 sensitivity of quantification. In fact, as reducing agents and amino acids are normally present in the
1085 conjugation reaction, the results from the BCA method are prone to being interfered and the
1086 Bradford method appears to be more suitable. On the contrary, the Bradford method needs to be
1087 performed in an acidic environment that is not appropriate for samples with poor stability or poor
1088 solubility in an acidic pH. Besides, the BCA method is more sensitive than the Bradford method
1089 (Kruger, 2009).

1090 Maya *et al* carried out a standard example of the application of the BCA to quantify conjugated anti-
1091 EGFR ligands on NPs. In their study, the authors developed cetuximab-conjugated chitosan NPs to
1092 deliver paclitaxel onto EGFR-overexpressing tumors and used the BCA to confirm the presence and
1093 determine the efficiency of cetuximab conjugation. The conjugated NPs were incubated with the BCA
1094 reagent and the absorbance of the obtained solution was firstly recorded at 562 nm and
1095 subsequently compared to that of the calibration curve. The results showed that the Cet conjugation
1096 efficiency was $42 \pm 6 \%$ for this study (Maya *et al.*, 2013).

1097 In our team, we use the Bradford assay as our daily control of ligand conjugation. In our previous
1098 publication, we used the Bradford method to estimate the amount of anti-EGFR scFv fragments that
1099 were successfully conjugated onto our SPIONs. Due to the binding ability of the Bradford's reagent to
1100 the kappa light chains present on scFv fragments, this method was suitable for scFv detection and
1101 quantification. The absorbance of the incubated samples with the reagent was measured at 630 nm
1102 and the concentration of the grafted scFv ($\mu\text{g/mL}$) was determined using a calibration curve (scFv
1103 concentrations of 0; 2.5; 5; 10; 15; 20; 25 $\mu\text{g/mL}$) with scFv-free SPIONs as the negative control. The
1104 results showed that around 13 targeting scFv fragments per NP were introduced onto our SPIONs
1105 (Vinh Nguyen *et al.*, 2020). In another study, Houdaihed and colleagues also used the Bradford
1106 method to confirm the presence and quantify the amount of the grafted anti-EGFR Fab fragments
1107 onto their polymeric NPs. A similar number of grafted ligands to our study was found in this study,
1108 with approximately 12 conjugated ligands per NP (Houdaihed *et al.*, 2020).

1109 In conclusion, a broad range of analytical methods can be used to confirm the success of ligand
1110 bioconjugation from simple methods to sophisticated ones. In addition to "daily control" such as
1111 changes in size and charge of finalized NPs compared to initial NPs, other analytical methods are
1112 highly recommended to provide a clear and precise confirmation. The choice of appropriate methods
1113 can be made according to the kind of ligands and NPs. As an example, if ligands are protein-based, it
1114 is useful to apply SDS-PAGE and protein dosage as complementary methods to size-charge controls in
1115 order to have both qualitative and quantitative information on conjugated ligands.

1116

1117

1118

1119

1120 **Table 4 Main analytical methods used for the detection of conjugated anti-EGFR ligands on NPs surface**

Analytical method	Qualitative/ Quantitative	Appropriate cases	Advantages	Drawbacks	References
Size and charge measurements	Qualitative	Increase in size (antibody-conjugation); changes in zeta potential (conjugation using electrostatic interactions)	Easy procedure; regular control	Lack of relevance	(Liu <i>et al.</i> , 2019; Lu <i>et al.</i> , 2018; Maya <i>et al.</i> , 2013; Wang and Zhou, 2015; Zhang <i>et al.</i> , 2012; Y. Zhang <i>et al.</i> , 2018)
FT-IR		Organic ligands on inorganic NPs; chemical conjugation strategies		Limited applications to organic ligands on inorganic NPs and chemical conjugation; low sensibility if the conjugation efficiency is not sufficient, and demand for a good purification method to eliminate non-reacted ligands	(Chen <i>et al.</i> , 2016; Lucky <i>et al.</i> , 2016; Y. Zhang <i>et al.</i> , 2018)
Thermogravimetric analysis		Organic ligands on inorganic NPs		Limited applications to organic ligands on inorganic NPs	(Marega <i>et al.</i> , 2016)
Elemental analysis techniques		Ligand-conjugated monomer for NMR; organic ligands on inorganic NPs for XPS		Limited applications to organic ligands on inorganic NPs; invasive method	(Marega <i>et al.</i> , 2016; Nan, 2019; Yamamoto <i>et al.</i> , 2019)
Fluorescence spectroscopy and imaging	Qualitative or semi-quantitative	All kinds of ligands and NPs	More selective and illustrating method;	A second fluorescence-labeled antibody or a	(Lu <i>et al.</i> , 2018; Lv <i>et al.</i> , 2018; Xie <i>et</i>

			possibility for quantification	labeled-ligand is required, a good purification method to eliminate non-reacted ligands is needed	<i>al.</i> , 2019)
SDS page gel electrophoresis	Qualitative or semi-quantitative	Protein-based ligands	The most used method for detecting of protein-based ligands; possibility to be used as a semi-quantitative method	Not suitable for non-protein ligands	(Gill <i>et al.</i> , 2018; Kao <i>et al.</i> , 2013; Zhai <i>et al.</i> , 2015)
Protein dosage	Quantitative	Protein-based ligands	Sensitive method for protein-based ligand (BCA assay); easiest and fastest method (within few minutes for the Bradford assay)	BCA is interfered by reducing agents, chelators and certain amino acids. The Bradford method needs to be performed in an acidic pH	(Houdaihed <i>et al.</i> , 2020; Maya <i>et al.</i> , 2013; Vinh Nguyen <i>et al.</i> , 2020)

1121

1122 **5. Conclusions**

1123 Nanoparticles functionalized with EGFR-targeting ligands are becoming an interesting field of study in
1124 the quest for better treatment of various types of cancer. The overexpression of EGFRs in various
1125 types of solid tumors makes them one of the most promising oncomarkers for targeted nanotherapy.
1126 Therefore, several types of anti-EGFR ligands with high binding affinity have been developed for
1127 nano-functionalization including the EGF protein and its derivatives, whole antibodies or antibody
1128 fragments, peptides and aptamers. The functionalization of NPs with these fragments offers many
1129 advantages including i) an enhancement in cancer cellular uptake via EGFR receptor-mediated
1130 endocytosis, ii) a higher *in vivo* tumor accumulation and retention level of loaded agents resulting in
1131 better therapeutic efficacy, iii) less systemic toxicity thanks to tumor targeting properties or
1132 neutralizing effects for highly charged NPs, and iv) possibility to be used spontaneously as
1133 therapeutic agents and as active targeting ligands.

1134 Despite these promising benefits, nanomedicines targeted with EGFR-targeted ligands should be
1135 designed to meet i) the pathophysiology of the disease due to possible mutations in the oncomarker
1136 and ii) the individual need of each patient in terms of drug content that we call “personalized
1137 nanomedicine”. Moreover, physicochemical properties, and the safety of nanomedicines should be
1138 also meticulously considered to better exploit the EPR effect (enhanced permeability and retention
1139 effect), and to address the risk of nano-toxicity.

1140 Secondly, as there is a strict correlation between the type, the number and the conformation of the
1141 conjugated ligands and the therapeutic efficiency, these aspects need to be optimized. One of the
1142 solutions to address these issues is to use an appropriate conjugation strategy. A variety of
1143 conjugation methods including both physical interactions and chemical reactions have been
1144 developed for the introduction of EGFR-targeting ligands onto NPs. As each conjugation method
1145 presents both advantages and drawbacks, the choice of a conjugation strategy should be considered
1146 regarding i) the type of NPs and targeting ligands, ii) their stability in reactive media or biological
1147 fluids and iii) eventual toxic byproducts. Among these methods, a selective conjugation method such
1148 as click chemistry is preferable. This method may not only help introduce a higher amount of ligands
1149 onto NPs but also control the orientation of the grafted ligands on the surface of NPs, resulting in
1150 better interactions between the ligands and their targets.

1151 After the conjugation, the presence of conjugated ligands need to be confirmed with suitable
1152 analytical methods. Currently, changes in colloidal properties of NPs after the conjugation remain the
1153 principal control of successful conjugation. However, the lack of relevance of this method needs to
1154 be underlined and more accurate methods should be more widely applied.

1155 Taken together, nanomedicines functionalized with EGFR-targeting ligands are remarkably promising
1156 for the cancer treatment but future optimization to obtain maximal therapeutic effects with minimal
1157 side effects is still needed.

1158 **References**

- 1159 Agarwal, P., Bertozzi, C.R., 2015. Site-Specific Antibody–Drug Conjugates: The Nexus of Bioorthogonal
1160 Chemistry, Protein Engineering, and Drug Development. *Bioconjug. Chem.* 26, 176–192.
1161 <https://doi.org/10.1021/bc5004982>
- 1162 Ahmad, Z.A., Yeap, S.K., Ali, A.M., Ho, W.Y., Alitheen, N.B.M., Hamid, M., 2012. scFv Antibody:
1163 Principles and Clinical Application. *Clin. Dev. Immunol.* 2012, 1–15.
1164 <https://doi.org/10.1155/2012/980250>
- 1165 Akbarzadeh Khiavi, M., Safary, A., Barar, J., Ajoolahady, A., Somi, M.H., Omid, Y., 2020.
1166 Multifunctional nanomedicines for targeting epidermal growth factor receptor in colorectal
1167 cancer. *Cell. Mol. Life Sci.* 77, 997–1019. <https://doi.org/10.1007/s00018-019-03305-z>
- 1168 Alibakhshi, A., Abarghooi Kahaki, F., Ahangarzadeh, S., Yaghoobi, H., Yarian, F., Arezumand, R.,
1169 Ranjbari, J., Mokhtarzadeh, A., de la Guardia, M., 2017a. Targeted cancer therapy through
1170 antibody fragments-decorated nanomedicines. *J. Controlled Release* 268, 323–334.
1171 <https://doi.org/10.1016/j.jconrel.2017.10.036>
- 1172 Alibakhshi, A., Abarghooi Kahaki, F., Ahangarzadeh, S., Yaghoobi, H., Yarian, F., Arezumand, R.,
1173 Ranjbari, J., Mokhtarzadeh, A., de la Guardia, M., 2017b. Targeted cancer therapy through
1174 antibody fragments-decorated nanomedicines. *J. Controlled Release* 268, 323–334.
1175 <https://doi.org/10.1016/j.jconrel.2017.10.036>
- 1176 Altintas, I., Heukers, R., van der Meel, R., Lacombe, M., Amidi, M., van Bergen en Henegouwen,
1177 P.M.P., Hennink, W.E., Schiffelers, R.M., Kok, R.J., 2013. Nanobody-albumin nanoparticles
1178 (NANAPs) for the delivery of a multikinase inhibitor 17864 to EGFR overexpressing tumor
1179 cells. *J. Controlled Release* 165, 110–118. <https://doi.org/10.1016/j.jconrel.2012.11.007>
- 1180 Arienti, C., Pignatta, S., Tesei, A., 2019. Epidermal Growth Factor Receptor Family and its Role in
1181 Gastric Cancer. *Front. Oncol.* 9, 1308. <https://doi.org/10.3389/fonc.2019.01308>
- 1182 Ashton, J.R., Gottlin, E.B., Patz, E.F., West, J.L., Badea, C.T., 2018. A comparative analysis of EGFR-
1183 targeting antibodies for gold nanoparticle CT imaging of lung cancer. *PLOS ONE* 13, e0206950.
1184 <https://doi.org/10.1371/journal.pone.0206950>
- 1185 Baselga, J., 2001. The EGFR as a target for anticancer therapy—focus on cetuximab. *Eur. J. Cancer* 37,
1186 16–22. [https://doi.org/10.1016/S0959-8049\(01\)00233-7](https://doi.org/10.1016/S0959-8049(01)00233-7)
- 1187 Biscaglia, F., Rajendran, S., Conflitti, P., Benna, C., Sommaggio, R., Litti, L., Mocellin, S., Bocchinfuso,
1188 G., Rosato, A., Palleschi, A., Nitti, D., Gobbo, M., Meneghetti, M., 2017. Enhanced EGFR
1189 Targeting Activity of Plasmonic Nanostructures with Engineered GE11 Peptide. *Adv. Healthc.*
1190 *Mater.* 6, 1700596. <https://doi.org/10.1002/adhm.201700596>
- 1191 Brinkman, A.M., Chen, G., Wang, Y., Hedman, C.J., Sherer, N.M., Havighurst, T.C., Gong, S., Xu, W.,
1192 2016. Aminoflavone-loaded EGFR-targeted unimolecular micelle nanoparticles exhibit anti-
1193 cancer effects in triple negative breast cancer. *Biomaterials* 101, 20–31.
1194 <https://doi.org/10.1016/j.biomaterials.2016.05.041>
- 1195 Byrne, J.D., Betancourt, T., Brannon-Peppas, L., 2008. Active targeting schemes for nanoparticle
1196 systems in cancer therapeutics. *Adv. Drug Deliv. Rev.* 60, 1615–1626.
1197 <https://doi.org/10.1016/j.addr.2008.08.005>
- 1198 Changavi, A.A., Shashikala, A., Ramji, A.S., 2015. Epidermal Growth Factor Receptor Expression in
1199 Triple Negative and Nontriple Negative Breast Carcinomas. *J. Lab. Physicians* 7, 079–083.
1200 <https://doi.org/10.4103/0974-2727.163129>
- 1201 Chariou, P.L., Lee, K.L., Wen, A.M., Gulati, N.M., Stewart, P.L., Steinmetz, N.F., 2015. Detection and
1202 Imaging of Aggressive Cancer Cells Using an Epidermal Growth Factor Receptor (EGFR)-
1203 Targeted Filamentous Plant Virus-Based Nanoparticle. *Bioconjug. Chem.* 26, 262–269.
1204 <https://doi.org/10.1021/bc500545z>
- 1205 Chen, J., Ouyang, J., Chen, Q., Deng, C., Meng, F., Zhang, J., Cheng, R., Lan, Q., Zhong, Z., 2017. EGFR
1206 and CD44 Dual-Targeted Multifunctional Hyaluronic Acid Nanogels Boost Protein Delivery to
1207 Ovarian and Breast Cancers In Vitro and In Vivo. *ACS Appl. Mater. Interfaces* 9, 24140–24147.
1208 <https://doi.org/10.1021/acsami.7b06879>

1209 Chen, Y., Wang, Jianjun, Wang, Jingshuai, Wang, L., Tan, X., Tu, K., Tong, X., Qi, L., 2016. Aptamer
1210 Functionalized Cisplatin-Albumin Nanoparticles for Targeted Delivery to Epidermal Growth
1211 Factor Receptor Positive Cervical Cancer. *J. Biomed. Nanotechnol.* 12, 656–666.
1212 <https://doi.org/10.1166/jbn.2016.2203>

1213 Chu, I.-M., Tseng, S.-H., Chou, M.-Y., 2015. Cetuximab-conjugated iron oxide nanoparticles for cancer
1214 imaging and therapy. *Int. J. Nanomedicine* 3663. <https://doi.org/10.2147/IJN.S80134>

1215 Ciardiello, F., Tortora, G., 2003. Epidermal growth factor receptor (EGFR) as a target in cancer
1216 therapy: understanding the role of receptor expression and other molecular determinants
1217 that could influence the response to anti-EGFR drugs. *Eur. J. Cancer* 39, 1348–1354.
1218 [https://doi.org/10.1016/S0959-8049\(03\)00235-1](https://doi.org/10.1016/S0959-8049(03)00235-1)

1219 Costa, R., Shah, A.N., Santa-Maria, C.A., Cruz, M.R., Mahalingam, D., Carneiro, B.A., Chae, Y.K.,
1220 Cristofanilli, M., Gradishar, W.J., Giles, F.J., 2017. Targeting Epidermal Growth Factor
1221 Receptor in triple negative breast cancer: New discoveries and practical insights for drug
1222 development. *Cancer Treat. Rev.* 53, 111–119. <https://doi.org/10.1016/j.ctrv.2016.12.010>

1223 Cui, J., Ju, Y., Houston, Z.H., Glass, J.J., Fletcher, N.L., Alcantara, S., Dai, Q., Howard, C.B., Mahler, S.M.,
1224 Wheatley, A.K., De Rose, R., Brannon, P.T., Paterson, B.M., Donnelly, P.S., Thurecht, K.J.,
1225 Caruso, F., Kent, S.J., 2019. Modulating Targeting of Poly(ethylene glycol) Particles to Tumor
1226 Cells Using Bispecific Antibodies. *Adv. Healthc. Mater.* 8, 1801607.
1227 <https://doi.org/10.1002/adhm.201801607>

1228 De Luca, A., Carotenuto, A., Rachiglio, A., Gallo, M., Maiello, M.R., Aldinucci, D., Pinto, A., Normanno,
1229 N., 2008. The role of the EGFR signaling in tumor microenvironment. *J. Cell. Physiol.* 214,
1230 559–567. <https://doi.org/10.1002/jcp.21260>

1231 Du, C., Qi, Y., Zhang, Y., Wang, Y., Zhao, X., Min, H., Han, X., Lang, J., Qin, H., Shi, Q., Zhang, Z., Tian, X.,
1232 Anderson, G.J., Zhao, Y., Nie, G., Yang, Y., 2018. Epidermal Growth Factor Receptor-Targeting
1233 Peptide Nanoparticles Simultaneously Deliver Gemcitabine and Olaparib To Treat Pancreatic
1234 Cancer with *Breast Cancer 2 (BRCA2)* Mutation. *ACS Nano* 12, 10785–10796.
1235 <https://doi.org/10.1021/acsnano.8b01573>

1236 Faucon, A., Benhelli-Mokrani, H., Fleury, F., Dutertre, S., Tramier, M., Boucard, J., Lartigue, L.,
1237 Nedellec, S., Hulin, P., Ishow, E., 2017. Bioconjugated fluorescent organic nanoparticles
1238 targeting EGFR-overexpressing cancer cells. *Nanoscale* 9, 18094–18106.
1239 <https://doi.org/10.1039/C7NR06533G>

1240 Gebauer, M., Skerra, A., 2020. Engineered Protein Scaffolds as Next-Generation Therapeutics. *Annu.*
1241 *Rev. Pharmacol. Toxicol.* 60, 391–415. <https://doi.org/10.1146/annurev-pharmtox-010818-021118>

1243 Gill, M.R., Menon, J.U., Jarman, P.J., Owen, J., Skaripa-Koukelli, I., Able, S., Thomas, J.A., Carlisle, R.,
1244 Vallis, K.A., 2018. ¹¹¹In-labelled polymeric nanoparticles incorporating a ruthenium-based
1245 radiosensitizer for EGFR-targeted combination therapy in oesophageal cancer cells.
1246 *Nanoscale* 10, 10596–10608. <https://doi.org/10.1039/C7NR09606B>

1247 Grapa, C.M., Mocan, T., Gonciar, D., Zdrehus, C., Mosteanu, O., Pop, T., Mocan, L., 2019. Epidermal
1248 Growth Factor Receptor and Its Role in Pancreatic Cancer Treatment Mediated by
1249 Nanoparticles. *Int. J. Nanomedicine* Volume 14, 9693–9706.
1250 <https://doi.org/10.2147/IJN.S226628>

1251 Holliger, P., Hudson, P.J., 2005. Engineered antibody fragments and the rise of single domains. *Nat.*
1252 *Biotechnol.* 23, 1126–1136. <https://doi.org/10.1038/nbt1142>

1253 Houdaihed, L., Evans, J.C., Allen, C., 2020. Dual-Targeted Delivery of Nanoparticles Encapsulating
1254 Paclitaxel and Everolimus: a Novel Strategy to Overcome Breast Cancer Receptor
1255 Heterogeneity. *Pharm. Res.* 37, 39. <https://doi.org/10.1007/s11095-019-2684-6>

1256 Huang, W.-T., Larsson, M., Wang, Y.-J., Chiou, S.-H., Lin, H.-Y., Liu, D.-M., 2015. Demethoxycurcumin-
1257 Carrying Chitosan–Antibody Core–Shell Nanoparticles with Multitherapeutic Efficacy toward
1258 Malignant A549 Lung Tumor: From in Vitro Characterization to in Vivo Evaluation. *Mol.*
1259 *Pharm.* 12, 1242–1249. <https://doi.org/10.1021/mp500747w>

1260 Ilkhani, H., Sarparast, M., Noori, A., Zahra Bathaie, S., Mousavi, M.F., 2015. Electrochemical
1261 aptamer/antibody based sandwich immunosensor for the detection of EGFR, a cancer
1262 biomarker, using gold nanoparticles as a signaling probe. *Biosens. Bioelectron.* 74, 491–497.
1263 <https://doi.org/10.1016/j.bios.2015.06.063>

1264 Jin, H., Pi, J., Zhao, Y., Jiang, J., Li, T., Zeng, X., Yang, P., Evans, C.E., Cai, J., 2017. EGFR-targeting PLGA-
1265 PEG nanoparticles as a curcumin delivery system for breast cancer therapy. *Nanoscale* 9,
1266 16365–16374. <https://doi.org/10.1039/C7NR06898K>

1267 Jokerst, J.V., Miao, Z., Zavaleta, C., Cheng, Z., Gambhir, S.S., 2011. Affibody-Functionalized Gold-Silica
1268 Nanoparticles for Raman Molecular Imaging of the Epidermal Growth Factor Receptor. *Small*
1269 7, 625–633. <https://doi.org/10.1002/smll.201002291>

1270 Jorge, S.E.D.C., Kobayashi, S.S., Costa, D.B., 2014. Epidermal growth factor receptor (EGFR) mutations
1271 in lung cancer: preclinical and clinical data. *Braz. J. Med. Biol. Res.* 47, 929–939.
1272 <https://doi.org/10.1590/1414-431X20144099>

1273 Juan, A., Cimas, F.J., Bravo, I., Pandiella, A., Ocaña, A., Alonso-Moreno, C., 2020. An Overview of
1274 Antibody Conjugated Polymeric Nanoparticles for Breast Cancer Therapy. *Pharmaceutics* 12,
1275 802. <https://doi.org/10.3390/pharmaceutics12090802>

1276 Kang, S.J., Jeong, H.Y., Kim, M.W., Jeong, I.H., Choi, M.J., You, Y.M., Im, C.S., Song, I.H., Lee, T.S., Park,
1277 Y.S., 2018. Anti-EGFR lipid micellar nanoparticles co-encapsulating quantum dots and
1278 paclitaxel for tumor-targeted theranosis. *Nanoscale* 10, 19338–19350.
1279 <https://doi.org/10.1039/C8NR05099F>

1280 Kao, H.-W., Lin, Y.-Y., Chen, C.-C., Chi, K.-H., Tien, D.-C., Hsia, C.-C., Lin, M.-H., Wang, H.-E., 2013.
1281 Evaluation of EGFR-targeted radioimmuno-gold-nanoparticles as a theranostic agent in a
1282 tumor animal model. *Bioorg. Med. Chem. Lett.* 23, 3180–3185.
1283 <https://doi.org/10.1016/j.bmcl.2013.04.002>

1284 Kim, G.P., Grothey, A., 2008. Targeting colorectal cancer with human anti-EGFR monoclonal
1285 antibodies: focus on panitumumab. *Biol. Targets Ther.* 2, 223–228.
1286 <https://doi.org/10.2147/btt.s1980>

1287 Kim, J., Lee, J., Choi, J.S., Kim, H.-S., 2018. Electrostatically assembled dendrimer complex with a high-
1288 affinity protein binder for targeted gene delivery. *Int. J. Pharm.* 544, 39–45.
1289 <https://doi.org/10.1016/j.ijpharm.2018.04.015>

1290 Kim, M.W., Jeong, H.Y., Kang, S.J., Choi, M.J., You, Y.M., Im, C.S., Lee, T.S., Song, I.H., Lee, C.G., Rhee,
1291 K.-J., Lee, Y.K., Park, Y.S., 2017. Cancer-targeted Nucleic Acid Delivery and Quantum Dot
1292 Imaging Using EGF Receptor Aptamer-conjugated Lipid Nanoparticles. *Sci. Rep.* 7, 9474.
1293 <https://doi.org/10.1038/s41598-017-09555-w>

1294 Kooijmans, S.A.A., Fliervoet, L.A.L., van der Meel, R., Fens, M.H.A.M., Heijnen, H.F.G., van Bergen en
1295 Henegouwen, P.M.P., Vader, P., Schiffelers, R.M., 2016. PEGylated and targeted extracellular
1296 vesicles display enhanced cell specificity and circulation time. *J. Controlled Release* 224, 77–
1297 85. <https://doi.org/10.1016/j.jconrel.2016.01.009>

1298 Kotagiri, N., Li, Z., Xu, X., Mondal, S., Nehorai, A., Achilefu, S., 2014. Antibody Quantum Dot
1299 Conjugates Developed via Copper-Free Click Chemistry for Rapid Analysis of Biological
1300 Samples Using a Microfluidic Microsphere Array System. *Bioconjug. Chem.* 25, 1272–1281.
1301 <https://doi.org/10.1021/bc500139u>

1302 Krasinskas, A.M., 2011. EGFR Signaling in Colorectal Carcinoma. *Pathol. Res. Int.* 2011, 932932.
1303 <https://doi.org/10.4061/2011/932932>

1304 Krishnamurthy, A., Jimeno, A., 2018. Bispecific antibodies for cancer therapy: A review. *Pharmacol.*
1305 *Ther.* 185, 122–134. <https://doi.org/10.1016/j.pharmthera.2017.12.002>

1306 Kruger, N.J., 2009. The Bradford Method For Protein Quantitation, in: Walker, J.M. (Ed.), *The Protein*
1307 *Protocols Handbook*. Humana Press, Totowa, NJ, pp. 17–24. https://doi.org/10.1007/978-1-59745-198-7_4

1309 Kwon, K.C., Ryu, J.H., Lee, J.-H., Lee, E.J., Kwon, I.C., Kim, K., Lee, J., 2014. Proteinticle/Gold Core/Shell
1310 Nanoparticles for Targeted Cancer Therapy without Nanotoxicity. *Adv. Mater.* 26, 6436–6441.
1311 <https://doi.org/10.1002/adma.201401499>

1312 Lee, J., Choi, Y., Kim, K., Hong, S., Park, H.-Y., Lee, T., Cheon, G.J., Song, R., 2010. Characterization and
1313 Cancer Cell Specific Binding Properties of Anti-EGFR Antibody Conjugated Quantum Dots.
1314 Bioconjug. Chem. 21, 940–946. <https://doi.org/10.1021/bc9004975>

1315 Lee, J., Kang, J.A., Ryu, Y., Han, S.-S., Nam, Y.R., Rho, J.K., Choi, D.S., Kang, S.-W., Lee, D.-E., Kim, H.-S.,
1316 2017. Genetically engineered and self-assembled oncolytic protein nanoparticles for targeted
1317 cancer therapy. Biomaterials 120, 22–31. <https://doi.org/10.1016/j.biomaterials.2016.12.014>

1318 Li, C., Cai, G., Song, D., Gao, R., Teng, P., Zhou, L., Ji, Q., Sui, H., Cai, J., Li, Q., Wang, Y., 2019.
1319 Development of EGFR-targeted evodiamine nanoparticles for the treatment of colorectal
1320 cancer. Biomater. Sci. 7, 3627–3639. <https://doi.org/10.1039/C9BM00613C>

1321 Li, J., Chen, L., Liu, N., Li, S., Hao, Y., Zhang, X., 2015a. EGF-coated nano-dendriplexes for tumor-
1322 targeted nucleic acid delivery *in vivo*. Drug Deliv. 1–8.
1323 <https://doi.org/10.3109/10717544.2015.1004381>

1324 Li, J., Li, S., Xia, S., Feng, J., Zhang, Xuedi, Hao, Y., Chen, L., Zhang, Xiaoning, 2015b. Enhanced
1325 transfection efficiency and targeted delivery of self-assembling h-R3-dendriplexes in EGFR-
1326 overexpressing tumor cells. Oncotarget 6, 26177–26191.
1327 <https://doi.org/10.18632/oncotarget.4614>

1328 Li, W., Liu, Z., Li, C., Li, N., Fang, L., Chang, J., Tan, J., 2016. Radionuclide therapy using ¹³¹I-labeled
1329 anti-epidermal growth factor receptor-targeted nanoparticles suppresses cancer cell growth
1330 caused by EGFR overexpression. J. Cancer Res. Clin. Oncol. 142, 619–632.
1331 <https://doi.org/10.1007/s00432-015-2067-2>

1332 Li, W., Wang, Y., Tan, S., Rao, Q., Zhu, T., Huang, G., Li, Z., Liu, G., 2018. Overexpression of Epidermal
1333 Growth Factor Receptor (EGFR) and HER-2 in Bladder Carcinoma and Its Association with
1334 Patients' Clinical Features. Med. Sci. Monit. 24, 7178–7185.
1335 <https://doi.org/10.12659/MSM.911640>

1336 Li, Z., Zhao, R., Wu, X., Sun, Y., Yao, M., Li, J., Xu, Y., Gu, J., 2005. Identification and characterization of
1337 a novel peptide ligand of epidermal growth factor receptor for targeted delivery of
1338 therapeutics. FASEB J. 19, 1978–1985. <https://doi.org/10.1096/fj.05-4058com>

1339 Lin, C.-Y., Yang, S.-J., Peng, C.-L., Shieh, M.-J., 2018. Panitumumab-Conjugated and Platinum-Cored
1340 pH-Sensitive Apoferritin Nanocages for Colorectal Cancer-Targeted Therapy. ACS Appl. Mater.
1341 Interfaces 10, 6096–6106. <https://doi.org/10.1021/acsami.7b13431>

1342 Liu, K.-C., Arivajagane, A., Wu, S.-J., Tzou, S.-C., Chen, C.-Y., Wang, Y.-M., 2019. Development of a
1343 novel thermal-sensitive multifunctional liposome with antibody conjugation to target EGFR-
1344 expressing tumors. Nanomedicine Nanotechnol. Biol. Med. 15, 285–294.
1345 <https://doi.org/10.1016/j.nano.2018.10.006>

1346 Lu, Q., Dai, X., Zhang, P., Tan, X., Zhong, Y., Yao, C., Song, M., Song, G., Zhang, Z., Peng, G., Guo, Z., Ge,
1347 Y., Zhang, K., Li, Y., 2018. Fe₃O₄@Au composite magnetic nanoparticles modified with
1348 cetuximab for targeted magneto-photothermal therapy of glioma cells. Int. J. Nanomedicine
1349 Volume 13, 2491–2505. <https://doi.org/10.2147/IJN.S157935>

1350 Lucky, S.S., Idris, N.M., Huang, K., Kim, J., Li, Z., Thong, P.S.P., Xu, R., Soo, K.C., Zhang, Y., 2016. *In vivo*
1351 Biocompatibility, Biodistribution and Therapeutic Efficiency of Titania Coated Upconversion
1352 Nanoparticles for Photodynamic Therapy of Solid Oral Cancers. Theranostics 6, 1844–1865.
1353 <https://doi.org/10.7150/thno.15088>

1354 Lv, T., Li, Z., Xu, L., Zhang, Y., Chen, H., Gao, Y., 2018. Chloroquine in combination with aptamer-
1355 modified nanocomplexes for tumor vessel normalization and efficient erlotinib/Survivin
1356 shRNA co-delivery to overcome drug resistance in EGFR-mutated non-small cell lung cancer.
1357 Acta Biomater. 76, 257–274. <https://doi.org/10.1016/j.actbio.2018.06.034>

1358 M. Cardoso, M., N. Peca, I., C. A. Roque, A., 2012. Antibody-Conjugated Nanoparticles for
1359 Therapeutic Applications. Curr. Med. Chem. 19, 3103–3127.
1360 <https://doi.org/10.2174/092986712800784667>

1361 Marabelle, A., Gray, J., 2015. Tumor-targeted and immune-targeted monoclonal antibodies: Going
1362 from passive to active immunotherapy: Tumor- and Immune-Targeted Monoclonal
1363 Antibodies. Pediatr. Blood Cancer 62, 1317–1325. <https://doi.org/10.1002/pbc.25508>

1364 Marega, R., Prasetyanto, E.A., Michiels, C., De Cola, L., Bonifazi, D., 2016. Fast Targeting and Cancer
1365 Cell Uptake of Luminescent Antibody-Nanozeolite Bioconjugates. *Small* 12, 5431–5441.
1366 <https://doi.org/10.1002/smll.201601447>

1367 Master, A.M., Sen Gupta, A., 2012. EGF receptor-targeted nanocarriers for enhanced cancer
1368 treatment. *Nanomed.* 7, 1895–1906. <https://doi.org/10.2217/nnm.12.160>

1369 Maya, S., Kumar, L.G., Sarmiento, B., Sanoj Rejinold, N., Menon, D., Nair, S.V., Jayakumar, R., 2013.
1370 Cetuximab conjugated O-carboxymethyl chitosan nanoparticles for targeting EGFR
1371 overexpressing cancer cells. *Carbohydr. Polym.* 93, 661–669.
1372 <https://doi.org/10.1016/j.carbpol.2012.12.032>

1373 Milane, L., Duan, Z., Amiji, M., 2011. Development of EGFR-Targeted Polymer Blend Nanocarriers for
1374 Combination Paclitaxel/Lonidamine Delivery To Treat Multi-Drug Resistance in Human Breast
1375 and Ovarian Tumor Cells. *Mol. Pharm.* 8, 185–203. <https://doi.org/10.1021/mp1002653>

1376 Muyldermans, S., 2013. Nanobodies: Natural Single-Domain Antibodies. *Annu. Rev. Biochem.* 82,
1377 775–797. <https://doi.org/10.1146/annurev-biochem-063011-092449>

1378 Nakagawa, S., Yoshida, S., Hirao, Y., Kasuga, S., Fuwa, T., 1985. Biological effects of biosynthetic
1379 human EGF on the growth of mammalian cells in vitro. *Differ. Res. Biol. Divers.* 29, 284–288.
1380 <https://doi.org/10.1111/j.1432-0436.1985.tb00328.x>

1381 Nan, Y., 2019. Lung carcinoma therapy using epidermal growth factor receptor-targeted lipid
1382 polymeric nanoparticles co-loaded with cisplatin and doxorubicin. *Oncol. Rep.*
1383 <https://doi.org/10.3892/or.2019.7323>

1384 Negahdari, B., Shahosseini, Z., Baniasadi, V., 2016. Production of human epidermal growth factor
1385 using adenoviral based system. *Res. Pharm. Sci.* 11, 43–48.

1386 Nelson, A.L., 2010. Antibody fragments: Hope and hype. *mAbs* 2, 77–83.
1387 <https://doi.org/10.4161/mabs.2.1.10786>

1388 Pi, J., Jiang, J., Cai, H., Yang, F., Jin, H., Yang, P., Cai, J., Chen, Z.W., 2017. GE11 peptide conjugated
1389 selenium nanoparticles for EGFR targeted oridonin delivery to achieve enhanced anticancer
1390 efficacy by inhibiting EGFR-mediated PI3K/AKT and Ras/Raf/MEK/ERK pathways. *Drug Deliv.*
1391 24, 1549–1564. <https://doi.org/10.1080/10717544.2017.1386729>

1392 ping, Y., Jian, Z., Yi, Z., Huoyu, Z., Feng, L., Yuqiong, Y., Shixi, L., 2010. Inhibition of the EGFR with
1393 nanoparticles encapsulating antisense oligonucleotides of the EGFR enhances radiosensitivity
1394 in SCCVII cells. *Med. Oncol.* 27, 715–721. <https://doi.org/10.1007/s12032-009-9274-0>

1395 Pyo, A., Yun, M., Kim, H.S., Kim, T.-Y., Lee, J., Kim, J.Y., Lee, S., Kwon, S.Y., Bom, H.-S., Kim, H.-S., Kim,
1396 D.-Y., Min, J.-J., 2018. ⁶⁴ Cu-Labeled Repebody Molecules for Imaging of Epidermal Growth
1397 Factor Receptor-Expressing Tumors. *J. Nucl. Med.* 59, 340–346.
1398 <https://doi.org/10.2967/jnumed.117.197020>

1399 Qian, Y., Qiu, M., Wu, Q., Tian, Y., Zhang, Y., Gu, N., Li, S., Xu, L., Yin, R., 2015. Enhanced cytotoxic
1400 activity of cetuximab in EGFR-positive lung cancer by conjugating with gold nanoparticles. *Sci.*
1401 *Rep.* 4, 7490. <https://doi.org/10.1038/srep07490>

1402 Ramakrishnan, M.S., Eswaraiyah, A., Crombet, T., Piedra, P., Saurez, G., Iyer, H., Arvind, A.S., 2009.
1403 Nimotuzumab, a promising therapeutic monoclonal for treatment of tumors of epithelial
1404 origin. *mAbs* 1, 41–48. <https://doi.org/10.4161/mabs.1.1.7509>

1405 Richards, D.A., Maruani, A., Chudasama, V., 2017. Antibody fragments as nanoparticle targeting
1406 ligands: a step in the right direction. *Chem. Sci.* 8, 63–77.
1407 <https://doi.org/10.1039/C6SC02403C>

1408 Roovers, R.C., Vosjan, M.J.W.D., Laeremans, T., el Khoulati, R., de Bruin, R.C.G., Ferguson, K.M.,
1409 Verkleij, A.J., van Dongen, G.A.M.S., van Bergen en Henegouwen, P.M.P., 2011. A biparatopic
1410 anti-EGFR nanobody efficiently inhibits solid tumour growth. *Int. J. Cancer* 129, 2013–2024.
1411 <https://doi.org/10.1002/ijc.26145>

1412 Sandoval, M.A., Sloat, B.R., Lansakara-P., D.S.P., Kumar, A., Rodriguez, B.L., Kiguchi, K., DiGiovanni, J.,
1413 Cui, Z., 2012. EGFR-targeted stearyl gemcitabine nanoparticles show enhanced anti-tumor
1414 activity. *J. Controlled Release* 157, 287–296. <https://doi.org/10.1016/j.jconrel.2011.08.015>

1415 Sasaki, T., Hiroki, K., Yamashita, Y., 2013. The Role of Epidermal Growth Factor Receptor in Cancer
1416 Metastasis and Microenvironment. *BioMed Res. Int.* 2013, 1–8.
1417 <https://doi.org/10.1155/2013/546318>

1418 Silva, C.O., Petersen, S.B., Reis, C.P., Rijo, P., Molpeceres, J., Fernandes, A.S., Gonçalves, O., Gomes,
1419 A.C., Correia, I., Vorum, H., Neves-Petersen, M.T., 2016. EGF Functionalized Polymer-Coated
1420 Gold Nanoparticles Promote EGF Photostability and EGFR Internalization for Photothermal
1421 Therapy. *PLOS ONE* 11, e0165419. <https://doi.org/10.1371/journal.pone.0165419>

1422 Specenier, P., Vermorken, J.B., 2013. Cetuximab: its unique place in head and neck cancer treatment.
1423 *Biol. Targets Ther.* 7, 77–90. <https://doi.org/10.2147/BTT.S43628>

1424 Sun, H., Zhu, X., Lu, P.Y., Rosato, R.R., Tan, W., Zu, Y., 2014. Oligonucleotide Aptamers: New Tools for
1425 Targeted Cancer Therapy. *Mol. Ther. - Nucleic Acids* 3, e182.
1426 <https://doi.org/10.1038/mtna.2014.32>

1427 Sun, H., Zu, Y., 2015. Aptamers and Their Applications in Nanomedicine. *Small* 11, 2352–2364.
1428 <https://doi.org/10.1002/smll.201403073>

1429 Talekar, M., Trivedi, M., Shah, P., Ouyang, Q., Oka, A., Gandham, S., Amiji, M.M., 2016. Combination
1430 wt-p53 and MicroRNA-125b Transfection in a Genetically Engineered Lung Cancer Model
1431 Using Dual CD44/EGFR-targeting Nanoparticles. *Mol. Ther.* 24, 759–769.
1432 <https://doi.org/10.1038/mt.2015.225>

1433 Teplinsky, E., Muggia, F., 2015. EGFR and HER2: is there a role in ovarian cancer? *Transl. Cancer Res.*
1434 Vol 4 No 1 Febr. 2015 *Transl. Cancer Res. Epithel. Ovarian Cancer Treat. Integrating Mol.*
1435 *Target.*

1436 Tonigold, M., Simon, J., Estupiñán, D., Kokkinopoulou, M., Reinholz, J., Kintzel, U., Kaltbeitzel, A.,
1437 Renz, P., Domogalla, M.P., Steinbrink, K., Lieberwirth, I., Crespy, D., Landfester, K., Mailänder,
1438 V., 2018. Pre-adsorption of antibodies enables targeting of nanocarriers despite a
1439 biomolecular corona. *Nat. Nanotechnol.* 13, 862–869. [https://doi.org/10.1038/s41565-018-](https://doi.org/10.1038/s41565-018-0171-6)
1440 [0171-6](https://doi.org/10.1038/s41565-018-0171-6)

1441 Tsai, W.-H., Yu, K.-H., Huang, Y.-C., Lee, C.-I., 2018. EGFR-targeted photodynamic therapy by
1442 curcumin-encapsulated chitosan/TPP nanoparticles. *Int. J. Nanomedicine* Volume 13, 903–
1443 916. <https://doi.org/10.2147/IJN.S148305>

1444 Vazquez-Lombardi, R., Phan, T.G., Zimmermann, C., Lowe, D., Jermutus, L., Christ, D., 2015.
1445 Challenges and opportunities for non-antibody scaffold drugs. *Drug Discov. Today* 20, 1271–
1446 1283. <https://doi.org/10.1016/j.drudis.2015.09.004>

1447 Venugopal, V., Krishnan, S., Palanimuthu, V.R., Sankarankutty, S., Kalaimani, J.K., Karupiah, S., Kit,
1448 N.S., Hock, T.T., 2018. Anti-EGFR anchored paclitaxel loaded PLGA nanoparticles for the
1449 treatment of triple negative breast cancer. In-vitro and in-vivo anticancer activities. *PLOS*
1450 *ONE* 13, e0206109. <https://doi.org/10.1371/journal.pone.0206109>

1451 Vinh Nguyen, P., Hervé-Aubert, K., David, S., Lautram, N., Passirani, C., Chourpa, I., Aubrey, N., Allard-
1452 Vannier, E., 2020. Targeted nanomedicine with anti-EGFR scFv for siRNA delivery into triple
1453 negative breast cancer cells. *Eur. J. Pharm. Biopharm.* S0939641120303040.
1454 <https://doi.org/10.1016/j.ejpb.2020.10.004>

1455 Walker, J.M., 2009. The Bicinchoninic Acid (BCA) Assay for Protein Quantitation, in: Walker, J.M. (Ed.),
1456 *The Protein Protocols Handbook*. Humana Press, Totowa, NJ, pp. 11–15.
1457 https://doi.org/10.1007/978-1-59745-198-7_3

1458 Wang, X.-B., Zhou, H.-Y., 2015. Molecularly targeted gemcitabine-loaded nanoparticulate system
1459 towards the treatment of EGFR overexpressing lung cancer. *Biomed. Pharmacother.* 70, 123–
1460 128. <https://doi.org/10.1016/j.biopha.2015.01.008>

1461 Wang, Yuyuan, Wang, Yidan, Chen, G., Li, Y., Xu, W., Gong, S., 2017. Quantum-Dot-Based Theranostic
1462 Micelles Conjugated with an Anti-EGFR Nanobody for Triple-Negative Breast Cancer Therapy.
1463 *ACS Appl. Mater. Interfaces* 9, 30297–30305. <https://doi.org/10.1021/acsami.7b05654>

1464 Wartlick, H., Michaelis, K., Balthasar, S., Strebhardt, K., Kreuter, J., Langer, K., 2004. Highly Specific
1465 HER2-mediated Cellular Uptake of Antibody-modified Nanoparticles in Tumour Cells. *J. Drug*
1466 *Target.* 12, 461–471. <https://doi.org/10.1080/10611860400010697>

1467 Wu, S.-C., Chen, Y.-J., Wang, H.-C., Chou, M.-Y., Chang, T.-Y., Yuan, S.-S., Chen, C.-Y., Hou, M.-F., Hsu,
1468 J.T.-A., Wang, Y.-M., 2016. Bispecific Antibody Conjugated Manganese-Based Magnetic
1469 Engineered Iron Oxide for Imaging of HER2/neu- and EGFR-Expressing Tumors. *Theranostics*
1470 6, 118–130. <https://doi.org/10.7150/thno.13069>

1471 Xie, X., Nie, H., Zhou, Y., Lian, S., Mei, H., Lu, Y., Dong, H., Li, F., Li, T., Li, B., Wang, J., Lin, M., Wang, C.,
1472 Shao, J., Gao, Y., Chen, J., Xie, F., Jia, L., 2019. Eliminating blood oncogenic exosomes into the
1473 small intestine with aptamer-functionalized nanoparticles. *Nat. Commun.* 10, 5476.
1474 <https://doi.org/10.1038/s41467-019-13316-w>

1475 Xu, J., Gattacceca, F., Amiji, M., 2013. Biodistribution and Pharmacokinetics of EGFR-Targeted
1476 Thiolated Gelatin Nanoparticles Following Systemic Administration in Pancreatic Tumor-
1477 Bearing Mice. *Mol. Pharm.* 10, 2031–2044. <https://doi.org/10.1021/mp400054e>

1478 Yamamoto, S., Iwamaru, Y., Shimizu, Y., Ueda, Y., Sato, M., Yamaguchi, K., Nakanishi, J., 2019.
1479 Epidermal growth factor-nanoparticle conjugates change the activity from anti-apoptotic to
1480 pro-apoptotic at membrane rafts. *Acta Biomater.* 88, 383–391.
1481 <https://doi.org/10.1016/j.actbio.2019.02.026>

1482 Yang, L., Mao, H., Wang, Y.A., Cao, Z., Peng, X., Wang, X., Duan, H., Ni, C., Yuan, Q., Adams, G., Smith,
1483 M.Q., Wood, W.C., Gao, X., Nie, S., 2009. Single chain epidermal growth factor receptor
1484 antibody conjugated nanoparticles for in vivo tumor targeting and imaging. *Small Weinh.*
1485 *Bergstr. Ger.* 5, 235–243. <https://doi.org/10.1002/sml.200800714>

1486 Yoo, J., Park, C., Yi, G., Lee, D., Koo, H., 2019. Active Targeting Strategies Using Biological Ligands for
1487 Nanoparticle Drug Delivery Systems. *Cancers* 11, 640.
1488 <https://doi.org/10.3390/cancers11050640>

1489 Yook, S., Cai, Z., Lu, Y., Winnik, M.A., Pignol, J.-P., Reilly, R.M., 2015. Radiation Nanomedicine for
1490 EGFR-Positive Breast Cancer: Panitumumab-Modified Gold Nanoparticles Complexed to the
1491 β -Particle-Emitter, ¹⁷⁷Lu. *Mol. Pharm.* 12, 3963–3972.
1492 <https://doi.org/10.1021/acs.molpharmaceut.5b00425>

1493 Yoon, A.-R., Kasala, D., Li, Y., Hong, J., Lee, W., Jung, S.-J., Yun, C.-O., 2016. Antitumor effect and
1494 safety profile of systemically delivered oncolytic adenovirus complexed with EGFR-targeted
1495 PAMAM-based dendrimer in orthotopic lung tumor model. *J. Controlled Release* 231, 2–16.
1496 <https://doi.org/10.1016/j.jconrel.2016.02.046>

1497 Yu, M.K., Park, J., Jon, S., 2012. Targeting strategies for multifunctional nanoparticles in cancer
1498 imaging and therapy. *Theranostics* 2, 3–44. <https://doi.org/10.7150/thno.3463>

1499 Zhai, J., Scoble, J.A., Li, N., Lovrecz, G., Waddington, L.J., Tran, N., Muir, B.W., Coia, G., Kirby, N.,
1500 Drummond, C.J., Mulet, X., 2015. Epidermal growth factor receptor-targeted lipid
1501 nanoparticles retain self-assembled nanostructures and provide high specificity. *Nanoscale* 7,
1502 2905–2913. <https://doi.org/10.1039/C4NR05200E>

1503 Zhang, P., Zhang, Y., Gao, M., Zhang, X., 2016. Dendrimer-assisted hydrophilic magnetic nanoparticles
1504 as sensitive substrates for rapid recognition and enhanced isolation of target tumor cells.
1505 *Talanta* 161, 925–931. <https://doi.org/10.1016/j.talanta.2016.08.064>

1506 Zhang, X., Yin, Liu, Ma, Wang, Hao, 2012. A novel EGFR-targeted gene delivery system based on
1507 complexes self-assembled by EGF, DNA, and activated PAMAM dendrimers. *Int. J.*
1508 *Nanomedicine* 4625. <https://doi.org/10.2147/IJN.S30671>

1509 Zhang, Y., Zhao, N., Qin, Y., Wu, F., Xu, Z., Lan, T., Cheng, Z., Zhao, P., Liu, H., 2018. Affibody-
1510 functionalized Ag₂S quantum dots for photoacoustic imaging of epidermal growth factor
1511 receptor overexpressed tumors. *Nanoscale* 10, 16581–16590.
1512 <https://doi.org/10.1039/C8NR02556H>

1513 Zhang, Z., Qian, H., Huang, J., Sha, H., Zhang, H., Yu, L., Liu, B., Hua, D., Qian, X., 2018. Anti-EGFR-iRGD
1514 recombinant protein modified biomimetic nanoparticles loaded with gambogic acid to
1515 enhance targeting and antitumor ability in colorectal cancer treatment. *Int. J. Nanomedicine*
1516 Volume 13, 4961–4975. <https://doi.org/10.2147/IJN.S170148>

1517 Zhou, Y., Drummond, D.C., Zou, H., Hayes, M.E., Adams, G.P., Kirpotin, D.B., Marks, J.D., 2007. Impact
1518 of Single-chain Fv Antibody Fragment Affinity on Nanoparticle Targeting of Epidermal Growth

1519 Factor Receptor-expressing Tumor Cells. *J. Mol. Biol.* 371, 934–947.
1520 <https://doi.org/10.1016/j.jmb.2007.05.011>
1521 Zimmermann, M., Zouhair, A., Azria, D., Ozsahin, M., 2006. The epidermal growth factor receptor
1522 (EGFR) in head and neck cancer: its role and treatment implications. *Radiat. Oncol.* 1, 11.
1523 <https://doi.org/10.1186/1748-717X-1-11>
1524

